Expression of clock genes tracks daily and tidal time in brains of intertidal crustaceans *Eurydice pulchra* and *Parhyale hawaiensis*

Oliphant, A. [1]*, Sia, C.Y. [1]*, Kyriacou, C.P. [2], Wilcockson, D.C. [3], Hastings, M.H. [1]

* Equal contribution.

[1]MRC Laboratory of Molecular Biology, Cambridge, CB2 0QH, UK

[2]Department of Genetics, Genomics and Cancer Sciences, University of Leicester, Leicester LE1 7RH, UK

[3]Department of Life Sciences, Aberystwyth University, Aberystwyth SY23 3DA, UK

ORCiD

AO	0000-0002-4867-5352
CYS	0009-0004-1138-000X
CPK	0000-0003-4889-7606
DCW	0000-0002-5923-4472
MHH	0000-0001-8576-6651

Abstract

Intertidal organisms, such as the crustaceans *Eurydice pulchra* and *Parhyale hawaiensis*, express daily and tidal rhythms of physiology and behaviour to adapt to their temporally complex environments. Although the molecular-genetic basis of the circadian clocks driving daily rhythms in terrestrial animals is well understood, the nature and mechanism of the circatidal clocks driving tidal rhythms remain a mystery. Using *in situ* hybridisation, we identified discrete clusters of ~60 putative "clock" cells co-expressing canonical circadian clock genes with comparable distributions across the protocerebrum of *E. pulchra* and *P. hawaiensis* brains. In tidally rhythmic, field-collected *E. pulchra* sampled under a light:dark (LD) cycle, the expression of *period* (*per*) and *cryptochrome 2* (*cry2*) exhibited daily rhythms in particular cell groups (e.g., medioposterior cells) whereas *timeless* (*tim*) showed 12-hour rhythms in others (e.g., medial cells). In tidally rhythmic laboratory-reared *P. hawaiensis*, previously entrained to 12.4-hour cycles of agitation under LD and sampled under continuous darkness, several cell groups (e.g., medioposterior cells) exhibited circadian expression of *per* and *cry2*. In contrast, dorsal-lateral cells in the protocerebrum exhibited robust ~12-hour, i.e., circatidal, rhythms of *per* and *cry2*, phased to the prior tidal agitation but not the prior LD. In *P. hawaiensis* exhibiting daily behaviour under LD without tidal agitation, robust daily rhythms of *per* and *cry2* expression were evident in medioposterior and other cells whereas expression in dorsal-lateral cells was not rhythmic, underlining their intrinsic tidal periodicity. These results implicate canonical circadian mechanisms in circatidal time-keeping and reveal conserved brain networks as potential neural substrates for the generation of interactive daily and tidal rhythms appropriate to intertidal habitats.

58

59 **Introduction:**

60

61 Organisms adapt to their cyclical environments through rhythms of metabolism, physiology
62 and behaviour that are driven by internal biological clocks [1]. Terrestrial environmental cycles
63 are predominantly daily, leading to the evolution of clocks with an autonomous period of
64 approximately one day (hence *circa-dian*) and entrained to the cycle of light and darkness. In
65 contrast, coastal environments present greater temporal complexity and marine organisms
66 have additionally evolved a range of circatidal (~12.4 hours), circasemilunar (~14.8 days) and
67 circalunar (~29.5 days) timing mechanisms [2 3] that co-ordinate adaptive rhythms across these
68 time domains. Despite their biological relevance, the mechanistic underpinnings of circatidal
69 clocks remain a mystery and three principal hypotheses have been proposed [2]. First, circatidal
70 and circadian rhythms are driven by a single oscillatory system the period of which is plastic,
71 adapting to the period of the dominant environmental cue [4]. Second, paired circalunidian
72 (~24.8-hour, i.e., slightly modified circadian) oscillators run in antiphase to create 12.4-hour
73 rhythms [5]. Third, separate 12.4-hour and 24-hour oscillators co-exist, independently driving
74 circatidal and daily phenotypes [6]. Testing these models requires identification of the clock
75 cells and genes responsible for tidal time-keeping.

76

77 Circadian clocks in animals pivot around a transcriptional/ translational feedback loop (TTFL)
78 in which positive factors CLOCK (CLK) and BMAL1 (or CYC in flies), acting through E-box
79 promotor sites, transactivate genes that encode negative regulators, PERIOD (PER),
80 CRYPTOCHROME2 (CRY2) and/ or TIMELESS (TIM), depending on species [7]. Accumulating
81 negative regulators progressively suppress transactivation and following their degradation the
82 cycle restarts after ~24 hours [8 9]. The intertidal isopod *Eurydice pulchra* and amphipod
83 *Parhyale hawaiensis* can express autonomous circadian and/ or circatidal rhythms of
84 locomotor behaviour in the absence of environmental cues [10 11 12 13]. However, the only
85 molecular markers of circatidal timekeeping relate to mitochondrial gene expression and
86 cellular redox state in *E. pulchra* [14]. Nevertheless, genes encoding CLOCK, BMAL1, PER and
87 CRY2 are present in both species [12 15] and *tim* expression in the head of *E. pulchra* is circadian
88 [12 16] (*P. hawaiensis* lacks *tim* [15]). *E. pulchra* CLOCK:BMAL1 heterodimers can transactivate
89 E-boxes and are suppressed by PER and CRY2 [12], whilst PhBMAL1 co-expressed with mouse
90 CLK can also transactivate E-boxes [13]. Finally, genomic deletion (*P. hawaiensis*) or RNAi-
91 knock-down (*E. pulchra*) of *Bmal1* compromises tidal activity rhythms[13 16], raising the intriguing
92 possibility of interactions between circadian and circatidal clocks at the molecular-genetic
93 level.

94

The current aim was to describe the expression of *Bmal1*, *Clk*, *per* and *cry2* (together with *Eptim*) across the brain to identify putative “clock” cells, and then to test their relationship to daily, circadian and circatidal behaviour. We reveal ~60 such cells arranged in multiple, discrete cell groups in the brain and show that particular groups are capable of tracking daily/ circadian time, encoded as the rhythmic expression of canonical circadian genes. Furthermore, we also identify cells with 12-hour rhythms of expression of *tim* in *E. pulchra* and of *per* and *cry2* in *P. hawaiensis* and show that the latter are capable of tracking circatidal time. These results implicate canonical circadian mechanisms in circatidal time-keeping. They also reveal brain networks that may be neural substrates for the generation of interactive daily and tidal rhythms appropriate to local intertidal habitats.

108 **Results**

109

110 ***Cellular expression of circadian clock genes in the brains of* E. pulchra *and* P.**
111 **hawaiensis.**

112 To map gene expression across the brain, we first generated reference brains for *E. pulchra*
113 and *P. hawaiensis* by averaging confocal image stacks of brains immunolabelled with anti-
114 SYNORF1 (Supplementary Figure 1). We segmented the neuropils to facilitate description of
115 gross brain anatomy and naming of clock cell groups relative to the body axis (Supplementary
116 Figure 2, Supplementary video 1, 2). Our neuroanatomical descriptions of *E. pulchra* are
117 based on the isopod *Saduria entomon* [17]. The brain structure of *P. hawaiensis* has been
118 described [18 19].

119

120 *Bmal1* is implicated in circadian and circatidal timekeeping in both *E. pulchra* and *P.*
121 *hawaiensis*. We therefore used whole-mount HCR-FISH to map *Bmal1* transcripts as a first
122 step to identify putative "clock" cells. This revealed widespread expression across the brain
123 of *E. pulchra* (Supplementary Figure 3A) and, consistent with qPCR studies [12], its intensity did
124 not change over time in LD (Supplementary Figure 4A). The expression of *Clk* mRNA was
125 similarly widespread in the brain of *E. pulchra*, with most cells expressing low levels although
126 there was a condensation of higher intensity signals in ~60 cells, located principally in the
127 median protocerebrum (Supplementary Figure 3B). These *Bmal1* and *Clk* expression patterns
128 in *E. pulchra* were confirmed using RNAscope™ on brain sections (Supplementary Figure 5).

129

130 Pan-cellular expression of *Bmal1* was also evident in the brain of *P. hawaiensis*
131 (Supplementary Figure 3C) and, again, this did not change across the light:dark (LD) cycle
132 (Supplementary Figure 4B). In contrast, the expression of *Clk* in *P. hawaiensis* was less
133 widespread than in *E. pulchra*, with enrichment in cells in the median protocerebrum
134 (Supplementary Figure 3D). The enrichment was clearer than in *E. pulchra* and these
135 enriched cells were comparable in number and location to those in *E. pulchra*. Thus,
136 notwithstanding the requirement for *Bmal1* to sustain circatidal behaviour in both species [13 16],
137 the pattern of its expression did not specifically signpost any populations of putative clock
138 cells. In contrast, the expression of *Clk* was significantly elevated in discrete cell populations
139 in the median protocerebrum of both species.

140

141 We then mapped the expression of genes encoding negative regulators: *per*, *cry2* and *tim*
142 across the brain of *E. pulchra*. This revealed strong, specific signal for all three transcripts
143 restricted to discrete cell clusters in the median protocerebrum (Supplementary Figure 3E, F,
144 G). In *P. hawaiensis* brain the expression of *per* and *cry2* exhibited a pattern similar to that of

145 *E. pulchra*, with high levels of both transcripts localised to ~60 cells in the median
146 protocerebrum (Supplementary Figure 3I, J). The HCR-FISH was specific, insofar as probes
147 against *deGFP* gave no signal Supplementary Figure 3H, K).
148
149
150 ***Co-expression of circadian clock genes in distinct cell groups of* E. pulchra *and* P.**
151 **hawaiensis *brains*.**
152 CLOCK:BMAL1 heterodimers are required for transactivation within the TTFL and so we
153 compared the co-expression of *Bmal1* and *Clk* by multiplexed HCR-FISH of *E. pulchra* brains
154 dissected in the light phase. The *Clk*-enriched cells expressed *Bmal1* at the low level seen in
155 other cells across the brain. They also expressed high levels of *per* (Figure 1A) and the *per*-
156 expressing cells also expressed *cry2* and *tim* (Figure 1B, C). Given that *per* and *cry2* encode
157 the principal negative regulators of E-box-mediated transcription in *E. pulchra* [12] this small
158 population of cells in the median protocerebrum co-expressed the full complement of genes
159 required for a functional TTFL, highlighting them as putative clock cells. Using a similar
160 approach in *P. hawaiensis* we found, again, that *Clk*-enriched cells expressed *Bmal1* and high
161 levels of *cry2* (Figure 1D). Furthermore, the *cry2*-enriched (and hence, *Clk*-enriched) cells
162 also expressed *per* (Figure 1E), indicating that they are likely TTFL-competent cells. By
163 combining HCR-FISH with anti-SYNORF1 immunofluorescence (Supplementary Figure 6,
164 Supplementary video 1, 2) the putative clock cell clusters were registered to the reference
165 brains (Figure 2). The groups were named by general location: 8 in *E. pulchra* and 9 in *P.*
166 *hawaiensis*, with a total of ~30 cells per hemisphere, distributed symmetrically (Supplementary
167 Table 1, Supplementary Results).
168
169
170 ***Rhythmic expression of circadian clock genes in circatidally rhythmic* E. pulchra *under***
171 ***a light:dark cycle.***
172 When placed into free-running conditions (DD) in the laboratory, field-collected *E pulchra*
173 displayed strong circatidal activity rhythms, with peak activity corresponding to the expected
174 time of high water on the home beach (Supplementary Figure 7). Across 11 independent field
175 collections, 54.5 ±6.5% of animals were tidally rhythmic (range: 20–76%) with a mean period
176 of 12.36 ±0.02 h (±SEM, N =478). To test whether some or all putative clock cells of *E. pulchra*
177 can track daily or tidal time, we performed whole-mount, multiplexed HCR-FISH on dissected
178 brains of circatidally rhythmic beach-collected *E. pulchra* sampled every 2 hours under LD
179 (16:8) for 24 hours (Figure 3A). The number of HCR-FISH spots was used to quantify
180 transcript abundance, and we considered expression to be rhythmic only when Kruskal-Wallis/
181 ANOVA identified a significant time effect and both JTK_CYC [20] and RAIN [21] were significant

182 (p<0.05) at a period of 12 or 24 hours, for circatidal and daily rhythms, respectively. The
183 aggregated counts across all cells, as a measure of total brain expression, showed strong
184 daily rhythms for *per*, *cry2* and *tim*, with peak levels in the late dark phase (Figure 3B).
185 Aggregate levels of *tim* also showed a statistically significant 12-hour rhythm, although the
186 overall profiles for aggregate *per*, *cry2* and *tim* were similar and tracked daily time.
187
188 To explore whether circatidal and circadian behavioural phenotypes are generated by different
189 cell populations that contain ~12-hour and ~24-hour molecular timers, we analysed clock gene
190 expression at the level of individual cell groups. Of the 7 examined, 5 showed significant
191 rhythms of one or multiple transcripts (Supplementary Table 2). Daily patterning was evident
192 for *per* and *cry2* expression in the medioposterior cells with peaks in late night (Figure 3C, D),
193 whilst medial cells had a daily rhythm of *per* but a 12-hour rhythm of *tim* (Figure 3E, F).
194 Lateroposterior cells also had a significant 12-hour cycle of *tim* (Supplementary Figure 8B),
195 whereas *per* and *cry2* levels in these cells were not significantly rhythmic. In summary, in
196 circatidally behaving *E. pulchra* sampled under LD, aggregate expression of *per* and *cry2*
197 tracked daily time, whilst aggregate levels of *tim* were more complex, reflecting both daily and
198 circatidal time. When examined across distinct cell groups, daily cycles of *per* and *cry2* were
199 evident in 4 of 7 groups whilst a 12-hour, putative circatidal, pattern of *tim* expression was
200 detected in two. Thus, distinct cell groups in *E. pulchra* appear able to track either daily or
201 tidal time.
202
203
204 ***Rhythmic expression of circadian clock genes in circatidally active* P. hawaiensis*.***
205 To establish circatidal behavioural rhythms, *P. hawaiensis* laboratory-reared under a 12L:12D
206 cycle were entrained by a cycle of mechanical agitation for 2 hours every 12.4 hours for >30
207 days. On transfer to free-running conditions of DD and no further agitation, they showed
208 circatidal rhythms with peak activity phased to anticipated agitation (i.e., subjective high-tide)
209 (Supplementary Figure 9A, B). Across 13 experiments, 52.8 ±2.8% of animals showed
210 circatidal behaviour (range 40 –70%) with a mean period of 12.40 ±0.02 h (±SEM, N =456)
211 (Supplementary Figure 9C, D). To confirm that the circatidal behaviour was phased by the
212 agitation and not by the LD cycle, a sub-group of animals were subjected to a phase-shifted
213 regime for the final 6 days of entrainment in which agitation occurred every 12.9 hours rather
214 than every 12.4 hours as in matched controls. It therefore accumulated a relative delay of ~6
215 hours (0.5 hours per cycle over ~12 cycles). On release to DD, control and phase-shifted
216 animals exhibited circatidal behavioural rhythms with peak activity at projected high tide and
217 periods of ~12.4 h that were not significantly different between groups (Kolmogorov-Smirnov
218 test: D =0.1779, p =0.59, n.s) (Supplementary Figure 9E, F, G). Over four replications of the

219 control and shifted regimes, their effectiveness (45.7% vs. 49.8% circatidal animals) was
220 comparable (paired t-test: t =0.27, df =3, p =0.80, n.s., Cohen's d =0.136). Importantly, the
221 phase of the circatidal behaviour was delayed by 4.94 ±0.51 h (±SEM, N =4) in phase-shifted
222 animals, relative to the controls (Supplementary Figure 9E, F, H). This not only confirms the
223 capacity of *P. hawaiensis* to exhibit circatidal behaviour [13] but it also demonstrates that the
224 circatidal clockwork of *P. hawaiensis* is sensitive to mechanical agitation, as is the case for *E.*
225 *pulchra* [11].
226
227 To test whether cells in *P. hawaiensis* could track circadian and/ or tidal time, whole-mount
228 HCR-FISH was applied to the brains of animals entrained by tidal agitation and exhibiting
229 circatidal activity before harvest (Figure 4A). Aggregate expression of *per* was circadian,
230 peaking in subjective night, whilst aggregate expression of *cry2* did not vary with time (Figure
231 4B). Across the 10 cell groups examined, 3 showed significant rhythms of one or multiple
232 transcripts (Supplementary Table 3). Notably, expression of *per* was strongly circadian in
233 medioposterior cells and anterior-medial a1 cells (Figure 4C, D and E, F). Moreover, these
234 cells also showed circadian cycles of *cry2* expression, running in antiphase to *per*. Thus, *per*
235 and *cry2* expression in these cells tracked circadian time rather than tidal time in circatidally
236 rhythmic animals. In contrast, dorsal-lateral cells in the same animals showed a significant
237 12-hour cycle of *per* and *cry2* transcripts (Figure 4G, H). Furthermore, in the dorsal-lateral
238 cells, unlike the circadian cells, *per* and *cry2* oscillated almost in phase, both peaking after
239 subjective high tide (~CT00-03 and CT15).
240
241 The experiment was repeated with the final tidal agitation occuring slightly later (+1.2 hours)
242 relative to the LD cycle. The animals exhibited robust circatidal activity rhythms, phased to
243 anticipated high water (Figure 5A). Aggregate expression of *per* was again circadian
244 (Supplementary Figure 10A). Across the 10 cell groups examined, the same three showed
245 significant rhythms of one or multiple transcripts (Supplementary Table 4). The expression of
246 *per* and *cry2* in the medioposterior and anterior-medial a1 cells was circadian (Supplementary
247 Figure 10B, C and D, E) whilst the dorsal-lateral cells again showed a strong circatidal, 12-
248 hour, pattern of expression of *per* and *cry*. The transcripts were also oscillating in phase and
249 peaking after subjective high tide (Figure 5B, C). To test whether we could phase-shift these
250 putative tidal cells even further, and to differentiate them from circadian cells exhibiting bimodal
251 24-hour rhythms, we entrained animals such that the final bout of tidal agitation occurred 5.4
252 hours phase-shifted relative to the 12:12LD cycle (i.e., subjective high tide at ~CT3.8 and
253 ~CT16.2). On release into constant conditions, the animals exhibited appropriately phased
254 circatidal rhythms of activity peaking at subjective high tide (Figure 5A). The aggregate
255 expression of *per* (but not *cry2*) was circadian, peaking in subjective night (Supplementary

256 Figure 11A). Of the 10 cell groups examined, 4 (the original three plus anterior-lateral cells)
257 showed an effect of time on transcript levels (Supplementary Table 5). Medioposterior cells
258 showed antiphasic circadian rhythms of *per* and *cry2*, anterior-medial a1 cells showed a
259 circadian cycle of *per* (Supplementary Figure 11B, C and D, E) and anterior-lateral cells were
260 circadian for *cry2*. In contrast, the dorsal-lateral cells again showed 12-hour cycles of
261 expression of *per* and *cry2* (Figure 5D, E). Moreover, the peaks occurred after subjective high
262 tide and therefore the profiles were phase-shifted relative to the prior LD cycle by ~6 hours
263 when compared to the previous tidal experiments. Comparison across the three experiments
264 with circatidally active animals showed conservation of the phase relationship between *per*
265 and *cry2* expression as well as adoption of the phase of the prior regime of tidal agitation
266 (Supplementary Figure 12). Thus, in the same brains of *P. hawaiensis* exhibiting free-running
267 circatidal behaviour, medioposterior and anterior-medial a1 cells consistently tracked
268 circadian time, expressed by antiphasic rhythms of *per* and *cry2* expression, whereas the
269 dorsal-lateral cells consistently tracked tidal time, independently of circadian time, and did so
270 with *per* and *cry2* rhythms in phase.
271
272
273 ***Rhythmic expression of circadian clock genes in daily-rhythmic* P. hawaiensis *under a***
274 ***light:dark cycle.***
275 To test whether dorsal-lateral cells have any capacity to follow daily time, we entrained *P.*
276 *hawaiensis* to LD cycles without tidal agitation. As reported [13] [10], *P. hawaiensis* exhibited
277 rhythmic activity under LD, peaking at night (Supplementary Figure 13A, B, D, E). Across 7
278 experiments 58.6 ±4.4% were rhythmic (range: 45 -80%, total N =189). When released into
279 constant darkness, ~50% of rhythmic animals (i.e., 22.9 ±7.5% of total), showed circadian
280 rhythms in their locomotor activity (Supplementary Figure 13A, C, D, F), with a mean (±SEM)
281 period of 24.17 ±0.17 h (N =39). Activity levels were significantly higher during the subjective
282 night than in the subjective day.
283
284 In animals confirmed to be showing daily behavioural activity prior to harvest of their brains
285 for HCR-FISH (Figure 6A), the aggregate expression of *per* was highly rhythmic, peaking at
286 night (Figure 6B). Aggregate expression of *cry2* was also significantly rhythmic, in antiphase
287 to *per*, but with a small amplitude. Of the 10 cell groups examined, 5 showed a daily pattern
288 of one or both transcripts (Supplementary Table 6). In both the medioposterior cell group and
289 the anterior-medial a1 cells, *per* and *cry2* were rhythmic and in antiphase, with nocturnal and
290 diurnal peaks, respectively (Figure 6C, D and E, F), echoing the circadian patterns seen in
291 these cells in tidally active animals under DD. Rhythmic expression of *per* was also evident
292 in the dorsal cells and the anterior-medial b cells (Supplementary Figure 14A, B and C, D),

again peaking in the night, and *cry2* was rhythmic in anterior-medial c cells. In contrast, there was no statistically significant rhythmic expression of either *per* or *cry2* in the dorsal-lateral cells of the daily-behaving animals (Figure 6G, H). Thus, several cell groups can exhibit daily cycles of gene expression in daily-behaving *P. hawaiensis* under LD, including the medioposterior and anterior-medial a1 cells that are also circadian under DD. In contrast, the circatidal gene expression observed in dorsal-lateral cells in tidally rhythmic animals under DD was specific to that condition: in the absence of tidal cues this population of cells did show tidal patterning, nor did they adopt the daily rhythms of expression seen in other cell groups under LD.

The distinctions between circadian and circatidal rhythms of gene expression are evident in a combined meta-analysis across the three tidal entrainment studies, registered alternatively in either circadian or circatidal time (Figure 7). When examined across all experiments in the same circatidally behaving animals, the expression of *per* and *cry2* was highly circadian in the medioposterior cells and anterior-medial a1 cells (Figure 7A, B), with *cry2* oscillating in anti-phase to *per*. On the other hand, the expression of *per* and *cry2* in dorsal-lateral cells was highly circatidal and co-phasic (Figure 7C). Circular plots registered to prior LD and tidal agitation emphasise these differences in periodicity and acrophase between the circadian and the circatidal cells (Figure 7D, E). Moreover, this mapping of the tidal oscillations to the phase of tidal entrainment in all three experiments confirmed that the dorsal-lateral cells were able to express a free-running molecular signature of tidal time that was independent of circadian time and revealed, thereby, that the brain of *P. hawaiensis* contains independent circadian and circatidally rhythmic cell populations.

318 **Discussion**

319

320 Examination of the expression of canonical circadian clock genes across the brains of both *E.*
321 *pulchra* and *P. hawaiensis* identified ~60 cells co-expressing *Clk*, *Bmal1*, *cry2* and *per*,
322 arranged into distinct groups across the protocerebrum. Although the loss of *Bmal1*
323 compromises circatidal behaviour in *E. pulchra* [16] and in *P. hawaiensis* [13], its brain-wide
324 expression showed no local enrichment and so did not highlight any potential circatidal clock
325 cells. This broad distribution is, however, consistent with BMAL1 having diverse, pleiotropic
326 actions beyond timekeeping [22]. On the other hand, the observed enrichment of *Clk*, *per*, and
327 *cry2* expression (alongside *tim* in *E. pulchra*) in specific cell groups indicated their potential
328 function as circadian oscillators.

329

330 In circatidally active *E. pulchra* sampled under LD cycles, the aggregated signals for *per* and
331 *cry2* were daily, reflective of their putative circadian roles, and both peaked in the late night as
332 expected for negative co-regulators within the TTFL. In contrast, aggregate brain expression
333 of *tim* showed significant patterning not only at 24 hours, consistent with circadian cycling of
334 *tim* in whole heads assayed by qPCR [12], but also at 12 hours. Analysis at the level of individual
335 cell groups provided a more granular insight, revealing 24-hour rhythms of *per* and *cry2* in
336 medioposterior cells and of *per* in medial cells, with peak expression in late night. This
337 absence of circatidal rhythmicity of *per* expression resonates with the finding that knockdown
338 of *per* to ~20% of wild-type levels, had no effect on circatidal activity in *E. pulchra*, although it
339 did disrupt circadian phenotypes [12]. Alternatively, *tim* showed 12-hour accumulation in both
340 the medial and the lateroposterior cells, peaking ~2 hours after expected high water. These
341 cell-specific differences in *tim* expression likely underlie the compound periodicity evident in
342 the aggregate expression. Furthermore, the 12-hour patterns in the medial and the
343 lateroposterior cells indicate potential tidal time-keeping in these cells associated with
344 circatidal behaviour.

345

346 In *P. hawaiensis*, aggregate expression of *per* tracked daily time under LD and circadian time
347 under DD, with elevated levels during the dark phase and subjective night, respectively. Daily
348 and circadian patterning was even more pronounced when examined in individual cell groups,
349 with rhythmic expression of *per* evident in medioposterior, anterior-medial a1, dorsal and
350 anterior-medial b cells. Notably, whereas *per* and *cry2* were in phase in daily cells of *E.*
351 *pulchra*, expression of *per* and *cry2* in daily and circadian cells in *P. hawaiensis* was antiphasic,
352 suggesting inter-species differences in the underlying molecular architecture of the circadian
353 TTFL.

354

355 Remarkably, following entrainment of *P. hawaiensis* to artificial tidal cycles under LD and then
356 subsequent transfer to free-running conditions, dorsal-lateral cells were robustly rhythmic for
357 *per* and *cry2* expression, with a circatidal period that reflected the circatidal behaviour of the
358 animals. Across independent trials, these cells tracked experimental tidal time, regardless of
359 prior LD phase. In contrast, clock gene expression in these cells was arrhythmic when
360 analysed across individuals sampled under LD without tidal cues and with daily, not tidal,
361 behaviour. These observations place the dorsal-lateral cells as strong candidates for
362 dedicated circatidal oscillators, especially when other cell groups in the same brains (e.g.,
363 medioposterior and anterior-medial a1 cells), ignored tidal cues and remained circadian,
364 phased to prior LD. Notably, *per* and *cry2* in these tidal cells oscillated in phase, in contrast
365 to the antiphasic rhythms of *per* and *cry2* in daily/ circadian cells. The functional significance
366 of these varying relationships, which are surprising in terms of the canonical TTFL whereby
367 *per* and *cry2* are co-phasic, is not clear but they suggest that a common molecular architecture
368 may have diverged, evolving to operate under different time-bases in different cells. Of the
369 canonical clock genes in *E. pulchra*, only *tim* expression was associated with tidal time in 2 of
370 the 4 neuronal groups studied. For *P hawaiensis* the non-canonical antiphasic expression of
371 *per* and *cry2* occurred in the circadian but not in the circatidal cells. Future analysis of protein
372 expression in these cell groups will better inform understanding of cell-specific TTFL
373 structures. In addition, examination of clock gene expression in the different cell groups of
374 animals with loss/ knock-down of BMAL1 (and CLK?) would indicate mechanistic bridges
375 between the TTFL and tidal behaviour. Nevertheless, it is possible that the circatidal
376 expression patterns of *Phper*, *Phcry2* and *Eptim* are driven by a cryptic tidal clock, such that
377 they reflect cellular activity but are not in themselves causal to tidal behaviour. The genetic
378 tractability of *P. hawaiensis* may enable this to be tested directly.
379
380 Notably, even though numerous cells oscillated at ~24 hours (22 in *P. hawaiensis*) and only a
381 few at ~12 hours (4 in *P. hawaiensis*), both *E. pulchra* and tidally entrained *P. hawaiensis* were
382 strongly circatidal in terms of behaviour. This raises the question of why strong tidal
383 phenotypes are reflected by relatively few tidal cells, compared to the strong aggregate cycles
384 of daily/ circadian gene expression. Of course, day/ night cycles are highly predictable in
385 nature, and it is therefore expected that circadian systems will be a prominent and robust
386 feature. Nevertheless, coastal animals have evolved temporally complex behaviours to match
387 their habitats [11] [12] [13] [10] cued by multiple stimuli. It is therefore possible that gene expression
388 may be circatidal in additional cell groups in *E. pulchra* and/ or *P. hawaiensis* but it evaded
389 statistical detection in the current study because of the high variance intrinsic to population-
390 based measures. Alternatively, it may be that different tidal cell groups respond to distinct
391 entraining cues and so only a subset of these groups is revealed in any single experimental

392 setting. Examination of gene expression in the brain of *P. hawaiensis* entrained by tidal
393 immersion/ emersion [13] with and without tidal agitation may indeed reveal additional putative
394 circatidal clock cells: can subsets of cells we describe here as non-rhythmic be recruited by
395 tidal stimuli of other modalities. Alternatively, it may emphasise the distinct and unique tidal
396 role of dorsal-lateral cells. Such a cell- and stimulus-specific entrainment repertoire raises the
397 question of how tidal stimuli are transduced to the central brain and whether a distributed
398 network broadens the capacity for tidal entrainment, reinforcing it in diverse natural settings [2]
399 [10] [11].
400
401 In considering the three hypotheses of circatidal time-keeping [4] [5] [6], our data concur most with
402 the model of dedicated tidal and daily timers proposed by Naylor [6], with canonical circadian
403 genes in distinct cell groups tuning to either circatidal or circadian periodicities. Our
404 demonstration that dual circatidal and circadian systems operate in parallel also corroborates
405 other work on circatidal clocks. For example, surgical removal of optic lobes of the mangrove
406 cricket, *Apteronemobius asahinai*, abrogates circadian but not circatidal locomotor
407 phenotypes, indicative of two anatomically separable timers [23] [24]. In contrast, evidence in
408 favour of a circadian/ tidal timer based on a single "plastic" clock, as proposed by Enright [4],
409 received support from studies on the coastal oyster *Crassostrea gigas*, which showed ~12-
410 hour and/ or ~24-hour expression of circadian gene homologues [25]. Importantly, these models
411 are not mutually exclusive. Given the evolutionary distance between molluscs and arthropods,
412 it is entirely possible that tidal time-keeping machineries have evolved independently. In fact,
413 a parsimonious explanation of the evolution of clock cells with different periodicities would be
414 that pre-existing circadian clock components were co-opted to track relevant tidal cues. The
415 cells we identified invariably co-expressed the rudiments of a circadian TTFL but with either
416 daily or tidal frequencies in the same brain and it is possible that they evolved in parallel,
417 diverging under the influence of photic and mechanosenory (tidal) inputs, respectively.
418
419 Kwiatkowski et al. [10] asked how *P. hawaiensis* 'chooses' between 12.4-hour and 24-hour
420 environmental rhythms during entrainment. Our observation that distinct circadian and
421 circatidal cells groups entrain independently to light and mechanical stimuli, respectively,
422 provides a solution to this problem. Similarly, the authors also questioned whether neurons
423 coordinating rhythmic behaviour in *P. hawaiensis* have two different timers with differential
424 sensitivity to light and tides, or two cell types exist. Whilst we cannot currently exclude the
425 former, our data align better with the latter. This does not preclude interactions of the two
426 systems, however, and the genetic and behavioural malleability of *P. hawaiensis* should
427 enable their decipherment. Thus, our findings may facilitate the examination of input and

output pathways of tidal and daily cues at cellular resolution, progressing towards defining the nature and connectivity of circadian and circatidal neural clockworks.

Acknowledgements

We thank Dr. Sebastian Cachero (LMB) and Dr. Gregory Jefferis (LMB) for their guidance on reference brain generation and their algorithms, as well as Dr. Aziz Aboobaker (Oxford) for providing a starting culture of Chicago-F *P. hawaiensis* and Dr. Michalis Averoff (Lyon) for advice on working with *P. hawaiensis*. We also thank the Mechanical and Electronics Workshops and the Light Microscopy Facility at the LMB for technical support. This work was supported by core funding from Medical Research Council (MRC), as part of United Kingdom Research and Innovation (also known as UK Research and Innovation) (MRC File Reference No. MC_U105170643) to M.H.H. C.Y.S. was supported by a Boehringer Ingelheim Fonds PhD fellowship (2023-2025). For the purpose of open access, the author has applied a CC BY public copyright licence to any Author Accepted Manuscript version arising.

Author contributions.

All Authors contributed to the direction of the project and the writing of the manuscript.
AO and CYS designed and conducted behavioural and neuroanatomical experiments and analysed data.
DCW conducted neuroanatomical experiments and analysed data.
MHH arranged funding.

458 **Methods**

459

460 ***Eurydice pulchra* collection and phenotypic analysis**

461 Animals were collected from Llanddona beach, Anglesey, UK, during spring high tides during
462 the months May to October [12]. Swimming behaviour of both females and males was recorded
463 in DAM10 and LAM10 activity monitors (Trikinetics Inc., USA) ambient lighting (LD) at 16°C
464 with animals housed individually in 3 ml (Ø: 11 mm) plastic vials containing 33 psu artificial
465 seawater (ASW, Reef Salt, Tropical Marine Centre, Germany) and ~5 mm depth of fine sand.
466 Infrared beam interruptions were recorded using the DAMSystem3 software (TriKinetics Inc.,
467 USA) in one-minute bins. The first peak in tidal swimming activity was omitted from analysis
468 and behavioural rhythmicity was assessed over the subsequent six tidal cycles using chi-
469 squared periodogram analysis in Rethomics R package [26].

470

471 ***Parhyale hawaiensis* husbandry and behavioural analysis**

472 Chicago F strain *P. hawaiensis* were maintained in 6.5 L polypropylene containers (h: 125 mm,
473 w: 260 mm, d: 260 mm) containing 30 –35 psu ASW and a layer of crushed coral substrate
474 (grain size 2 –20 mm). Animals were reared at 25°C under 12h light:dark (LD) cycles. The
475 containers were covered with clear Perspex lids to prevent evaporation and aerated using
476 aquarium air pumps and air stones. Animals were fed carrots, goldfish flakes (Tetra GmbH,
477 Germany), algae wafers (Kyorin Food Ind. Ltd., Japan), freeze-dried brine shrimps, and/or
478 freeze-dried Tubifex (Interpret, UK) once weekly. Full water changes were performed
479 fortnightly. For locomotor activity monitoring, female and male animals were placed
480 individually into 23 mL polystyrene vials (h: 75 mm, Ø: 23.5 mm) containing a layer (~2 mm)
481 of crushed coral substrate (grain size 2 –5 mm) and approximately 6 cm of 30 psu ASW at
482 25°C. Tubes were loosely covered with parafilm and loaded into two-tier activity monitors
483 modified from the LAM25 Locomotor Activity Monitors (TriKinetics Inc., USA; Supplementary
484 Figure 2a) configured to record swimming and/or roaming activity. Infrared beam interruptions
485 were recorded using the DAMSystem3 software (TriKinetics Inc., USA).

486

487 Beam interruptions were collected into 30-minute bins and normalised within each animal by
488 dividing the count in each bin by the average count across all bins for that animal.
489 Autocorrelation periodogram was used to determine whether animals were rhythmic, with a
490 significance threshold of $\alpha = 0.05$ [27]. The period and the power of rhythmicity were determined
491 using Lomb-Scargle periodogram analysis [28] of binned and normalised data at the significance
492 level $\alpha = 0.05$. For circatidal experiments, the first subjective high tide after loading was omitted
493 from analysis and behavioural rhythmicity was assessed over the subsequent six tidal cycles.

494 For circadian entrainment experiments, animals loaded into the monitor were subjected to at
495 least four 12:12 LD (ZT0/lights-on at 0600 local time) cycles before being allowed to free run
496 in DD. For tidal entrainment, animals were kept under LD as above but mechanically agitated
497 on an orbital shaker set at 50 –60 rpm for 2 hours at 12.4-hour intervals. For behavioural
498 monitoring, animals were taken from entrainment regimes during the agitation phase and
499 placed in the activity monitor as described above to free-run without agitation in DD.
500
501 **Brain collection and processing for immunohistochemistry and HCR-FISH**
502 Animals were anaesthetised in ice-cold seawater, and their brains dissected using sharpened
503 watch-maker's forceps in ice-chilled physiological saline [29] (*E. pulchra)* or 0.22 µm filter-
504 sterilised ASW (30 -35 psu, FASW; *P. hawaiensis*). Tissues were immediately fixed in 4%
505 paraformaldehyde (made in PBS for *E. pulchra* and FASW for *P. hawaiensis*) for 1 hour at
506 room temperature, dehydrated serially in 33%, 66%, 100% methanol in PBST (PBS
507 supplemented with 0.1% Tween20), and stored in 100% methanol at -20°C for at least 16 h
508 before hybridisation or immunohistochemistry. Immediately prior to use, brains were
509 rehydrated in 66/33% methanol and washed/equilibrated in PBST (3x10 min). Neuropils were
510 immunolabelled using anti-SYNORF1 antibody (3C11, Developmental Studies Hybridoma
511 Bank (DSHB)). For *E. pulchra* and *P. hawaiensis* brains immunohistochemistry followed [30], [31]
512 and (Supplementary Methods). HCR™RNA-FISH probes were designed and synthesised by
513 Molecular Instruments Inc, USA against user-supplied sequences (Supplementary Table 8).
514 HCR-FISH followed the manufacturer's protocol [32] with some minor alterations following [33]
515 (Supplementary Methods). To co-localise putative clock cells relative to major neuropils,
516 immunostaining with anti-SYNORF1 antibody was followed by HCR-FISH (Supplementary
517 Methods). Reference brains were generated from confocal image stacks of brains in which
518 neuropils were labelled with anti-SYNORF1 (Supplementary Methods).
519
520 **Time-course sampling design.**
521 To investigate clock gene expression pattern in the brain of *E. pulchra*, animals were collected
522 from Llanddona beach, Anglesey, UK, during spring high tides in October 2024 and loaded
523 into activity monitors. Prior to sampling, animals were maintained under 18 h: 6 h L:D cycle
524 for 24 hours. Animals showing peaks of swimming activity during the two subjective high
525 waters during this interval were sampled every two hours, beginning at ZT7 (Supplementary
526 Figure 15A). To investigate circatidal clock gene expression patterns in the brain of tidally
527 entrained *P. hawaiensis*, animals which had been subjected to tidal entrainment were loaded
528 into activity monitors as described. Sampling occurred every 3 hours, beginning at CT0 on
529 the day after monitor loading and ending at CT24, for a total of 9 timepoints (Supplementary
530 Figure 15B). Individuals were only sampled if they showed peaks of locomotor activity during

531 the subjective high tides preceding their sampling timepoint. To investigate daily clock gene
532 expression pattern in the brain of *P. hawaiensis*, animals were loaded into activity monitors
533 and subjected to 12 h: 12 h LD cycle for 6 days as described. Individuals showing significant
534 24-h rhythmicity in locomotor activity (as described) over this entrainment period up to the day
535 before sampling were marked for sampling. On the day of sampling, marked animals were
536 sampled every 2 hours, beginning at ZT1 and ending at ZT25, for a total of 13 timepoints
537 (Supplementary Figure 15C). Dissected brains were processed for digital HCR-FISH as
538 described. HCR-FISH probes used for time -course experiments are described in
539 Supplementary Table 10.
540
541 **Whole brain digital HCR-FISH**
542 For quantification of diffraction-limited spots [32], signal amplification with 60 nM of each hairpin
543 was performed for 1 h, followed by staining with 1 µg/mL DAPI (as above). Brains were
544 mounted in Prolong Glass Antifade Mountant (ThermoFisher #P36980). *E. pulchra* brains
545 were mounted with the posterior surface apposed to the coverslip whilst *P. hawaiensis* brains
546 were mounted with the anterior surface apposed. To minimise signal loss with imaging depth,
547 brains were compressed to within 40 µm by mounting the coverslips containing brains onto
548 spacers made from double-sided adhesive tape (Radio Spares #770-3422). An Andor BC43
549 CF benchtop microscope equipped with a 60x/1.42NA Plan Apochromat oil immersion
550 objective was used to image each brain with an optical section interval of 0.3 µm.
551
552 To prepare images for segmentation of cell groups enriched for expression of *per*, *cry2*, and/
553 or *Clk/ tim*, 2D maximum filters were applied to each HCR-FISH channel, followed by
554 summation of the filtered images across channels and 2D gaussian filtering. The resulting
555 images, together with the corresponding raw DAPI image as the auxiliary channel, were
556 subjected to segmentation using Cellpose [34] and a custom model (available at GitHub) trained
557 via the human-in-the-loop functionality of the Cellpose 2.0 graphical user interface [35]. The
558 resulting masks were manually curated as required in napari [36] and assigned to distinct cell
559 groups. For spot detection, images were deconvolved using ClearView™ Deconvolution with
560 10 iterations after being acquired in the Fusion software. RNA foci were then detected in
561 deconvolved images and assigned to cell groups using the RS-FISH ImageJ plugin [37].
562
563 **Statistical analyses**
564 Shapiro-Wilk test used to determine normal distribution of data, and Levene's test used to
565 determine if the variances of all groups are equal. An overall time effect was tested by ANOVA
566 for normally distributed data and by Kruskal-Wallis for non-normal datasets. Where this
567 yielded a statistically significant effect, rhythmicity in the data was analysed further by JTK

CYCLE [20] and RAIN [21] at 12-hour or 24-hour periods. JTK-cycle p-values are adjusted using Bonferroni's method, and RAIN p-values are adjusted using the adaptive Benjamini-Hochberg (default) method. Gene expression was considered rhythmic when ANOVA was significant, and both JTK CYCLE and RAIN were significant for the same period (12 hours or 24 hours).

References

1. Dunlap, J.C., Loros, J.J., and Decoursey, P.J. (2004). Chronobiology: biological timekeeping (Sinauer).
2. Naylor, E. (2010). Chronobiology of marine organisms (Cambridge University Press).
3. Hafker, N.S., Andreatta, G., Manzotti, A., Falciatore, A., Raible, F., and Tessmar-Raible, K. (2023). Rhythms and Clocks in Marine Organisms. Ann Rev Mar Sci *15*, 509-538. 10.1146/annurev-marine-030422-113038.
4. Enright, J.T. (1976). Plasticity in an isopod's clockworks: shaking shapes form and affects phase and frequency. Journal of Comparative Physiology A *107*, 13-37.
5. Palmer, J.D. (1997). Dueling hypotheses: circatidal versus circalunidian battle basics--second engagement. Chronobiol Int *14*, 431-433. 10.3109/07420529709001463.
6. Naylor, E. (1996). Crab clockwork: the case for interactive circatidal and circadian oscillators controlling rhythmic locomotor activity of *Carcinus maenas*. Chronobiol Int *13*, 153-161. 10.3109/07420529609012649.
7. Reppert, S.M., and Weaver, D.R. (2000). Comparing Clockworks: Mouse versus Fly. Journal of Biological Rhythms *15*, 357-364. 10.1177/074873000129001459.
8. Andreani, T.S., Itoh, T.Q., Yildirim, E., Hwangbo, D.S., and Allada, R. (2015). Genetics of Circadian Rhythms. Sleep Med Clin *10*, 413-421. 10.1016/j.jsmc.2015.08.007.
9. Hardin, P.E., and Panda, S. (2013). Circadian timekeeping and output mechanisms in animals. Curr Opin Neurobiol *23*, 724-731. 10.1016/j.conb.2013.02.018.
10. Kwiatkowski, E.R., Rosenthal, J.J.C., and Emery, P. (2024). Crosstalk between the circatidal and circadian clocks mediates behavioral adaptation to tidal patterns. Curr Biol *34*, 5239-5251 e5232. 10.1016/j.cub.2024.09.067.
11. Hastings, M.H. (1981). The Entraining Effect of Turbulence on the Circa-Tidal Activity Rhythm and Its Semi-Lunar Modulation in *Eurydice pulchra*. J Mar Biol Assoc Uk *61*, 151-160. Doi 10.1017/S0025315400045987.
12. Zhang, L., Hastings, M.H., Green, E.W., Tauber, E., Sladek, M., Webster, S.G., Kyriacou, C.P., and Wilcockson, D.C. (2013). Dissociation of circadian and circatidal timekeeping in the marine crustacean *Eurydice pulchra*. Curr Biol *23*, 1863-1873. 10.1016/j.cub.2013.08.038.
13. Kwiatkowski, E.R., Schnytzer, Y., Rosenthal, J.J.C., and Emery, P. (2023). Behavioral circatidal rhythms require Bmal1 in *Parhyale hawaiensis*. Curr Biol *33*, 1867-1882 e1865. 10.1016/j.cub.2023.03.015.
14. O'Neill, J.S., Lee, K.D., Zhang, L., Feeney, K., Webster, S.G., Blades, M.J., Kyriacou, C.P., Hastings, M.H., and Wilcockson, D.C. (2015). Metabolic molecular markers of the tidal clock in the marine crustacean *Eurydice pulchra*. Curr Biol *25*, R326-327. 10.1016/j.cub.2015.02.052.
15. Hunt, B.J., Mallon, E.B., and Rosato, E. (2019). In silico Identification of a Molecular Circadian System With Novel Features in the Crustacean Model Organism *Parhyale hawaiensis*. Front Physiol *10*, 1325. 10.3389/fphys.2019.01325.

16. Zhang, L., Green, E.W., Webster, S.G., Hastings, M.H., Wilcockson, D.C., and Kyriacou, C.P. (2023). Correction: The circadian clock gene bmal1 is necessary for co-ordinated circatidal rhythms in the marine isopod *Eurydice pulchra* (Leach). PLoS Genet *19*, e1011047. 10.1371/journal.pgen.1011047.
17. Kenning, M., and Harzsch, S. (2013). Brain anatomy of the marine isopod *Saduria entomon* Linnaeus, 1758 (Valvifera, Isopoda) with special emphasis on the olfactory pathway. Front Neuroanat *7*, 32. 10.3389/fnana.2013.00032.
18. Wittfoth, C., Harzsch, S., Wolff, C., and Sombke, A. (2019). The "amphi"-brains of amphipods: new insights from the neuroanatomy of *Parhyale hawaiensis* (Dana, 1853). Front Zool *16*, 30. 10.1186/s12983-019-0330-0.
19. Ramos, A.P., Gustafsson, O., Labert, N., Salecker, I., Nilsson, D.E., and Averof, M. (2019). Analysis of the genetically tractable crustacean *Parhyale hawaiensis* reveals the organisation of a sensory system for low-resolution vision. BMC Biol *17*, 67. 10.1186/s12915-019-0676-y.
20. Hughes, M.E., Hogenesch, J.B., and Kornacker, K. (2010). JTK_CYCLE: An Efficient Nonparametric Algorithm for Detecting Rhythmic Components in Genome-Scale Data Sets. Journal of Biological Rhythms *25*, 372-380. 10.1177/0748730410379711.
21. Thaben, P.F., and Westermark, P.O. (2014). Detecting Rhythms in Time Series with RAIN. Journal of Biological Rhythms *29*, 391-400. 10.1177/0748730414553029.
22. Zheng, Y., Pan, L., Wang, F., Yan, J., Wang, T., Xia, Y., Yao, L., Deng, K., Zheng, Y., Xia, X., et al. (2023). Neural function of Bmal1: an overview. Cell Biosci *13*, 1. 10.1186/s13578-022-00947-8.
23. Takekata, H., Numata, H., and Shiga, S. (2014). The circatidal rhythm persists without the optic lobe in the mangrove cricket *Apteronemobius asahinai*. J Biol Rhythms *29*, 28-37. 10.1177/0748730413516309.
24. Takekata, H., Numata, H., Shiga, S., and Goto, S.G. (2014). Silencing the circadian clock gene Clock using RNAi reveals dissociation of the circatidal clock from the circadian clock in the mangrove cricket. J Insect Physiol *68*, 16-22. 10.1016/j.jinsphys.2014.06.012.
25. Tran, D., Perrigault, M., Ciret, P., and Payton, L. (2020). Bivalve mollusc circadian clock genes can run at tidal frequency. Proc Biol Sci *287*, 20192440. 10.1098/rspb.2019.2440.
26. Geissmann, Q., Garcia Rodriguez, L., Beckwith, E.J., and Gilestro, G.F. (2019). Rethomics: An R framework to analyse high-throughput behavioural data. PLOS ONE *14*, e0209331. 10.1371/journal.pone.0209331.
27. Levine, J.D., Funes, P., Dowse, H.B., and Hall, J.C. (2002). Signal analysis of behavioral and molecular cycles. BMC Neuroscience *3*, 1. 10.1186/1471-2202-3-1.
28. Ruf, T. (1999). The Lomb-Scargle Periodogram in Biological Rhythm Research: Analysis of Incomplete and Unequally Spaced Time-Series. Biological Rhythm Research *30*, 178-201. 10.1076/brhm.30.2.178.1422.
29. Saver, M.A., Wilkens, J.L., and Syed, N.I. (1999). In Situ and In Vitro Identification and Characterization of Cardiac Ganglion Neurons in the Crab, *Carcinus maenas*. Journal of Neurophysiology *81*, 2964-2976. 10.1152/jn.1999.81.6.2964.
30. Ostrovsky, A., Cachero, S., and Jefferis, G. (2013). Clonal analysis of olfaction in Drosophila: immunochemistry and imaging of fly brains. Cold Spring Harb Protoc *2013*, 342-346. 10.1101/pdb.prot071720.

31. Meissner, G.W., Grimm, J.B., Johnston, R.M., Sutcliffe, B., Ng, J., Jefferis, G.S.X.E., Cachero, S., Lavis, L.D., and Malkesman, O. (2018). DPX Mounting of Drosophila CNS. protocols.io. dx.doi.org/10.17504/protocols.io.qj2duqe.
32. Choi, H.M.T., Schwarzkopf, M., Fornace, M.E., Acharya, A., Artavanis, G., Stegmaier, J., Cunha, A., and Pierce, N.A. (2018). Third-generation *in situ* hybridization chain reaction: multiplexed, quantitative, sensitive, versatile, robust. Development *145*, dev165753. 10.1242/dev.165753.
33. Bruce, H.S., Jerz G., Kelly, S.R., McCarthy, J., Pomerantz, A., Senevirathne, G., Sherrard, A., Sun, D.A., Wolff, C., Patel, N.H. (2021). Hybridization Chain Reaction (HCR) In Situ Protocol V.1 protocols.io. dx.doi.org/10.17504/protocols.io.bunznvf6.
34. Stringer, C., Wang, T., Michaelos, M., and Pachitariu, M. (2021). Cellpose: a generalist algorithm for cellular segmentation. Nat Methods *18*, 100-106. 10.1038/s41592-020-01018-x.
35. Pachitariu, M., and Stringer, C. (2022). Cellpose 2.0: how to train your own model. Nature Methods *19*, 1634-1641. 10.1038/s41592-022-01663-4.
36. Sofroniew, N., Lambert, T., Bokota, G., Nunez-Iglesias, J., Sobolewski, P., Sweet, A., Gaifas, L., Evans, K., Burt, A., Doncila Pop, D., et al. (2024). napari: a multi-dimensional image viewer for Python (v0.5.0) (Zenodo).
37. Bahry, E., Breimann, L., Zouinkhi, M., Epstein, L., Kolyvanov, K., Mamrak, N., King, B., Long, X., Harrington, K.I.S., Lionnet, T., and Preibisch, S. (2022). RS-FISH: precise, interactive, fast, and scalable FISH spot detection. Nature Methods *19*, 1563-1567. 10.1038/s41592-022-01669-y.

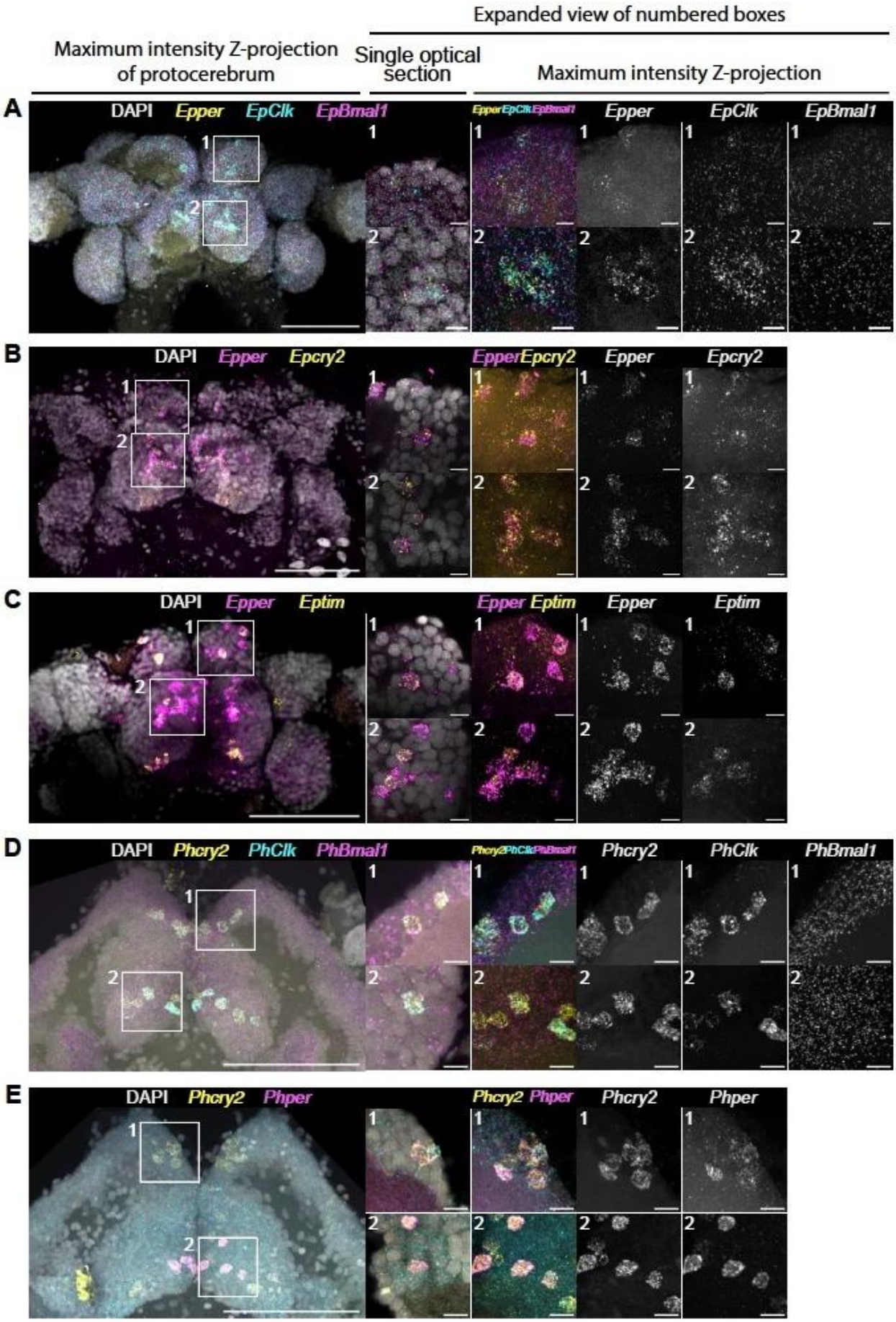
Expanded view of numbered boxes
Maximum intensity Z-projection of protocerebrum
Single optical section
Maximum intensity Z-projection
A
DAPI Epper EpClk EpBmal1
EpperEpClkEpBmal1
Epper
EpClk
EpBmal1
B
DAPI Epper Epcry2
EpperEpcry2
Epper
Epcry2
C
DAPI Epper Eptim
Epper Eptim
Epper
Eptim
D
DAPI Phcry2 PhClk PhBmal1
Phcry2PhClkPhBmal1
Phcry2
PhClk
PhBmal1
E
DAPI Phcry2 Phper
Phcry2 Phper
Phcry2
Phper

Figure 1. Cellular co-expression of circadian clock genes in the brains of *E. pulchra* and *P. hawaiensis*.

(A) Representative maximum intensity Z-projections and single optical sections of *E. pulchra* brain probed for *Epper*, *EpClk* and *EpBmal1* using HCR-FISH. Left: merged low-power (25x) view of protocerebrum of *E. pulchra*, centre: merged high-power (40x) single optical sections in boxes labelled 1 and 2, right: single channel high-power maximum intensity Z-projections. *EpBmal1* is widely and uniformly expressed in both putative clock cells and other cells across the brain, but it is not enriched in cells enriched for *EpClk*, whereas *Epper* is enriched in *EpClk*-enriched cells.

(B) As in A for *Epper* and *Epcry2*, expression of which is co-enriched in putative clock cells but not in other cells in the brain of *E. pulchra*.

(C) As in A for *Epper* and *Eptim*, of *Epper*-enriched cells in *E. pulchra*.

(D) As in A but for *P. hawaiensis* brain probed for *PhBmal1*, *PhClk* and *Phcry2* using HCR-FISH. *PhBmal1* is widely and uniformly expressed in both putative clock cells and other cells across the brain, but it is not enriched in cells enriched for *PhClk*, whereas *Phcry2* is enriched in *PhClk*-enriched cells.

(E) As in A but for *P. hawaiensis* brain labelled for *Phcry2* and *Phper*. *Phcry2* and *Phper* are co-enriched in putative clock cells, but not other cells in the brain.

Scale bars: 100 μm (left-most panels), 10 μm (other panels).

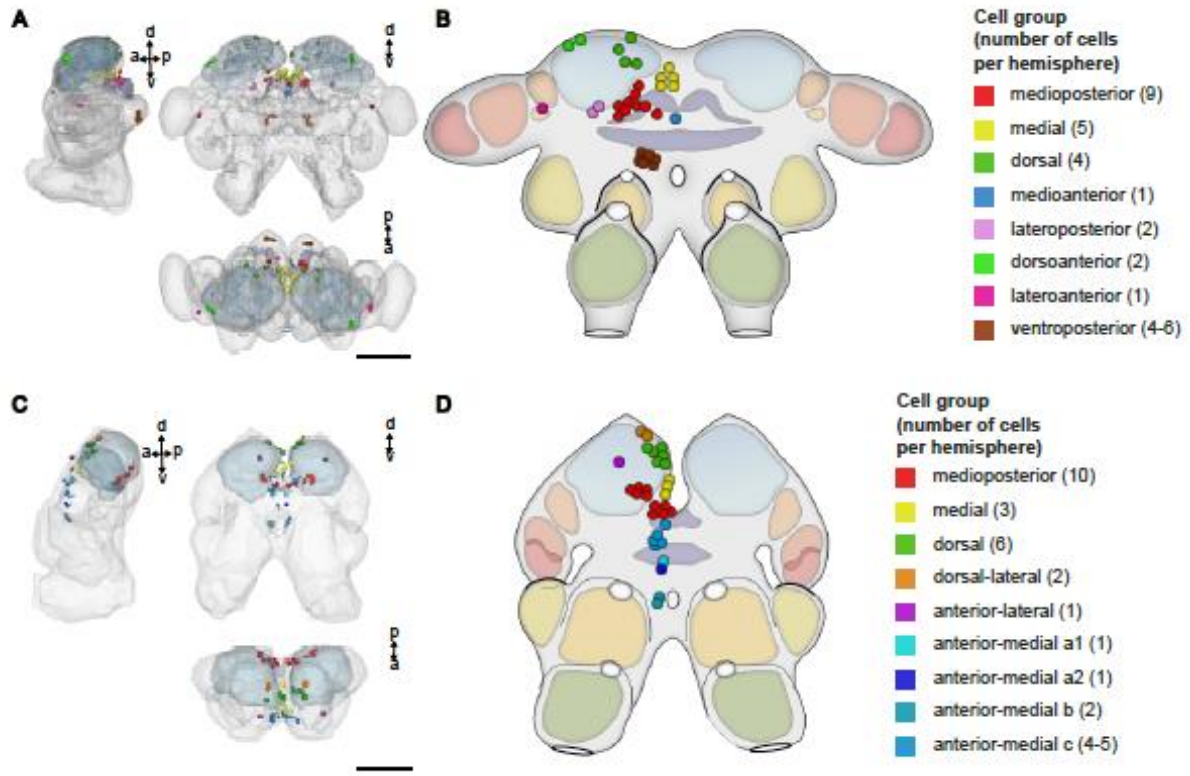

Figure 2. Putative clock cells in the brains of *E. pulchra* and *P. hawaiensis* revealed by co-expression of canonical circadian clock genes.

(A) Lateral, frontal and dorsal views of the *E. pulchra* reference brain model (from Supplementary Figure 2A) on to which somata enriched for expression of *Epper* and *Epcry2* are registered and segmented. The neuropils referred to in the Supplementary Materials (Supplementary Results) to signpost putative clock cells are here made translucent.

(B) Diagrammatic representation of the *E. pulchra* brain summarising the locations of cells co-enriched for *Epper* and *Epcry2*, based on the 3D reconstruction in A.

(C) Lateral, frontal and dorsal views of the *P. hawaiensis* reference brain model (from Supplementary Figure 2C) on to which somata enriched for expression of *Phper* and *Phcry2* are registered and segmented. The neuropils referred to in the Supplementary Materials (Supplementary Results) to signpost putative clock cells are here made translucent.

(D) Diagrammatic representation of the *P. hawaiensis* brain summarising the locations of cells co-enriched for *Phper* and *Phcry2*, based on the 3D reconstruction in C.

Compass markers in A and C show anterior (a), posterior (p), dorsal (d) and ventral (v) directions. Discrete cell groups are colour coded (see key). Cell numbers within each group (per hemisphere) in parenthesis. Scale bars: 100 µm.

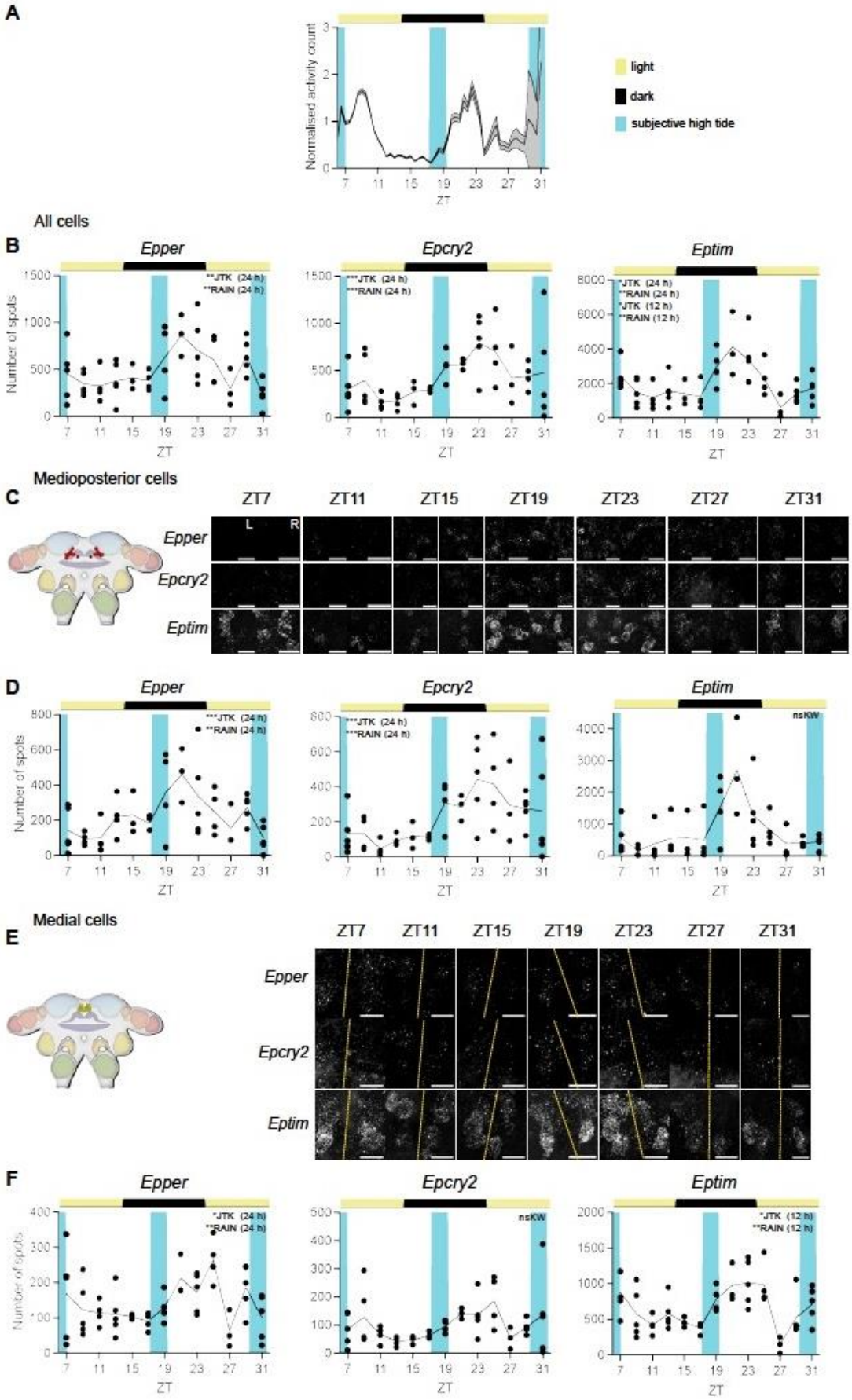
A
Normalised activity count
ZT
light
dark
subjective high tide
All cells
B
Epper
Epcry2
Eptim
Number of spots
ZT
**JTK (24 h)
**RAIN (24 h)
***JTK (24 h)
***RAIN (24 h)
*JTK (24 h)
**RAIN (24 h)
*JTK (12 h)
**RAIN (12 h)
Medioposterior cells
C
ZT7
ZT11
ZT15
ZT19
ZT23
ZT27
ZT31
L
R
Epper
Epcry2
Eptim
D
Epper
Epcry2
Eptim
Number of spots
ZT
***JTK (24 h)
**RAIN (24 h)
nsKW
Medial cells
E
ZT7
ZT11
ZT15
ZT19
ZT23
ZT27
ZT31
Epper
Epcry2
Eptim
F
Epper
Epcry2
Eptim
Number of spots
ZT
*JTK (24 h)
**RAIN (24 h)
nsKW
*JTK (12 h)
**RAIN (12 h)

Figure 3. Time course of expression of *per, cry2 and tim* in cells of tidally rhythmic *E. pulchra* held on a LD cycle.

(A) Normalised swimming activity (mean +SEM, shading) of beach-collected *E. pulchra* harvested under LD (16L:8D) for the HCR-FISH time-course (initial group size at start of harvest at ZT7 =65).

(B). Mean aggregate expression, quantified as the number of FISH spots, of *Epper, Epcry2* and *Eptim* across all cells plotted across time in beach-collected animals held under LD. Each point is from one brain.

(C) Left: cartoon to show location of medioposterior cell group in the brain. Right: representative maximum intensity Z-projections of *Epper*, *Epcry2* and *Eptim* expression in both hemispheres (L: left, R: right) across ZT (individual HCR-FISH channels in rows). Scale bars: 20 µm.

(D) Mean expression, quantified as the number of FISH spots, of *Epper* and *Epcry2* in medioposterior cell group plotted across time in beach-collected animals held under LD. Each point is from one brain.

(E, F) As C and D but for medial cells group. Yellow dashed lines: midlines. Scale bars: 10 µm.

Inset text indicates statistical tests (JTK-cycle and RAIN) performed to determine rhythmicity following significant time effect by ANOVA or Kruskall-Wallis. $p < 0.001$***, $p < 0.01$**, $p \leq 0.05$*, $p > 0.05^{ns}$. See also Supplementary Figure 8 for clock gene expression in lateroposterior cell group. For statistics and data shown in this figure, refer to Supplementary Table 2.

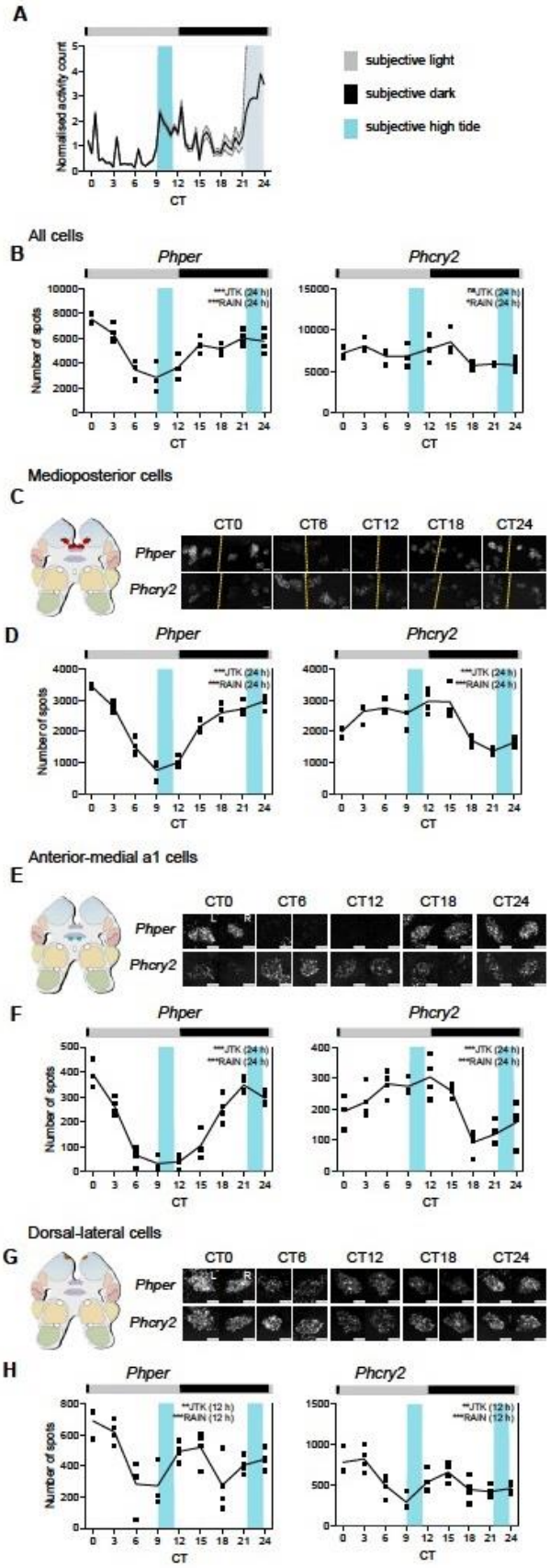
A
Normalised activity count
CT
subjective light
subjective dark
subjective high tide
All cells
B
Phper
Phcry2
Number of spots
***JTK (24 h)
***RAIN (24 h)
**JTK (24 h)
*RAIN (24 h)
Medioposterior cells
C
CT0
CT6
CT12
CT18
CT24
D
Anterior-medial a1 cells
E
F
Dorsal-lateral cells
G
H
**JTK (12 h)
***RAIN (12 h)

Figure 4. Free-running clock gene expression rhythms in tidally entrained *P. hawaiensis* (tidal phase θ).

(A) Normalised swimming activity (mean +SEM, shading) of *P. hawaiensis* synchronised to the prior agitation cycle and harvested for the HCR-FISH time-course (initial group size at start of harvest at CT0 =37).

(B) Mean aggregate expression, quantified as the number of FISH spots, of *Phper* and *Phcry2* across all putative clock cells plotted across time in tidally entrained animals sampled under DD. Each point is from one brain.

(C) Left: cartoon to show location of medioposterior cell group in the brain. Right: representative maximum intensity Z-projections of *Phper* and *Phcry2* expression in both hemispheres (L: left, R: right) across CT (individual HCR-FISH channels in rows). Scale bars: 5 µm.

(D) Plots of mean transcript abundance, quantified as the number of FISH spots, across CT for *Phper* (left) and *Phcry2* (right). Each point is from one brain.

(E, F) As in C and D for anterior-medial a1 cells. Yellow dashed lines: midlines. Scale bars: 10 µm.

(G, H) As in C and D for dorsal-lateral cells.

Inset text indicates statistical tests (JTK-cycle and RAIN) performed to determine 24-h and 12-h rhythmicity with the tested periods in parentheses. $p < 0.001^{***}$, $p < 0.01^{**}$, $p \leq 0.05^{*}$, $p > 0.05^{ns}$. For statistics shown in this figure, refer to Supplementary Table 3.

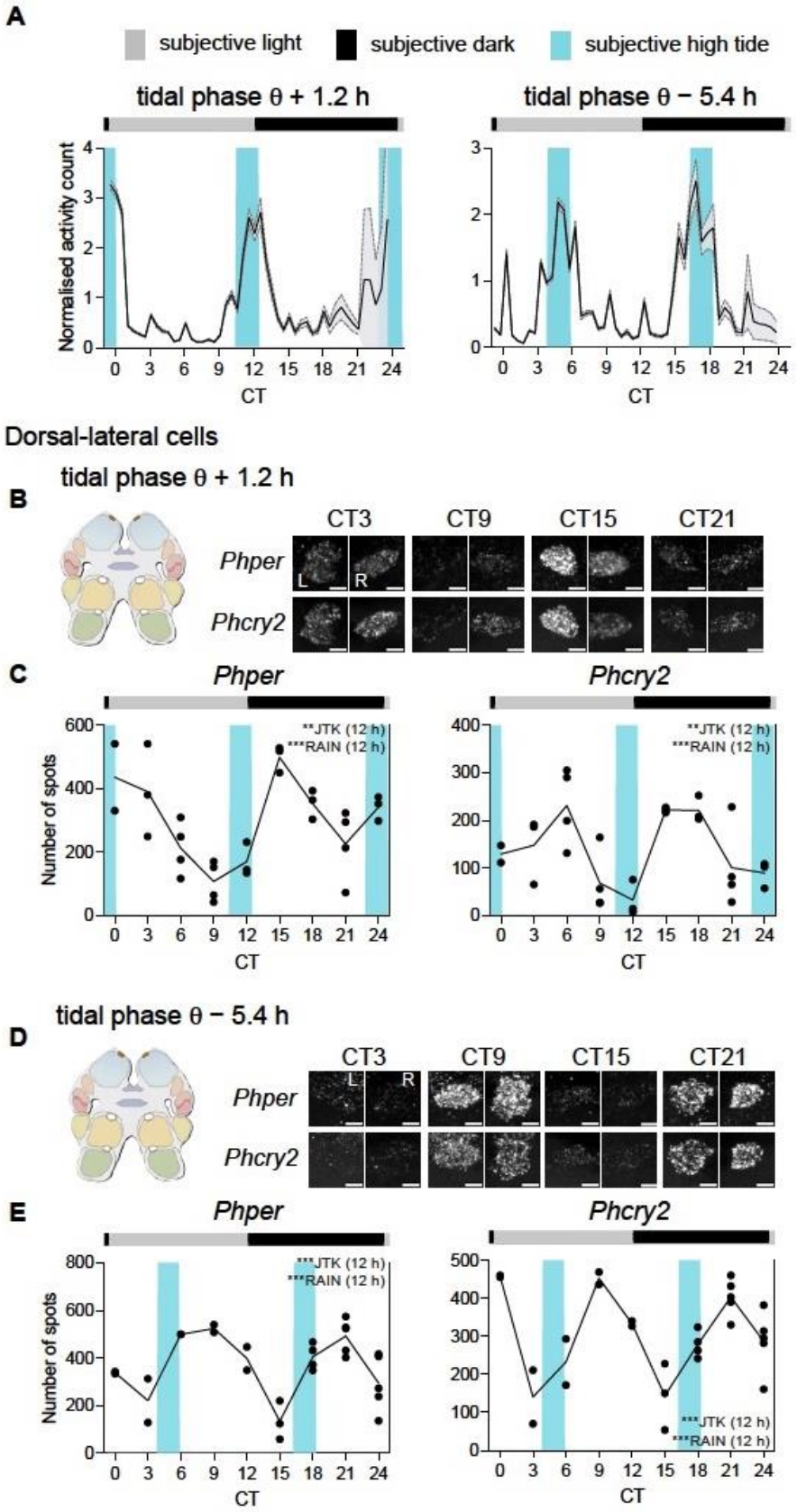
A
subjective light
subjective dark
subjective high tide
tidal phase θ + 1.2 h
tidal phase θ − 5.4 h
Normalised activity count
CT
Dorsal-lateral cells
B
tidal phase θ + 1.2 h
CT3
CT9
CT15
CT21
Phper
Phcry2
L
R
C
Phper
Phcry2
Number of spots
**JTK (12 h)
***RAIN (12 h)
D
tidal phase θ − 5.4 h
E
***JTK (12 h)
***RAIN (12 h)

Figure 5. **Circatidal rhythms of expression of *Phper*, *Phcry2* in dorsal-lateral cells in the brain of tidally entrained *P. hawaiensis*.**

(A) Normalised swimming activity (mean +SEM, shading) of *P. hawaiensis* synchronised to the prior agitation cycle, phase-shifted by +1.2 hours (left) or -5.4 hours (right) and harvested for the HCR-FISH time-course (initial group sizes at start of harvest at CT0 = 35).

(B) Left: cartoon to show location of dorsal-lateral cell group in the brain. Right: Representative maximum intensity Z-projections of *Phper* and *Phcry2* in both hemispheres (L: left, R: right) across CT (individual HCR-FISH channels in rows). Scale bars: 5 µm.

(C) Plots of mean transcript abundance, quantified as the number of FISH spots, across circadian time for *Phper* (left) and *Phcry2* (right) (blue shadings: subjective high water). Each point is from one brain.

(D, E) As in B and C for animals entrained to a tidal cycle advanced, relative to the LD cycle, by 5.4 hours.

Inset text indicates statistical tests (JTK-cycle and RAIN) performed to determine rhythmicity, with the tested periods in parentheses. p <0.001***, p< 0.01**, p ≤0.05*, p >0.05^{ns}. For statistics and data of FISH time-course experiments on tidally entrained animals, refer to Supplementary Table 4 and 5 for tidal phases θ +1.2 h and θ –5.4 h, respectively.

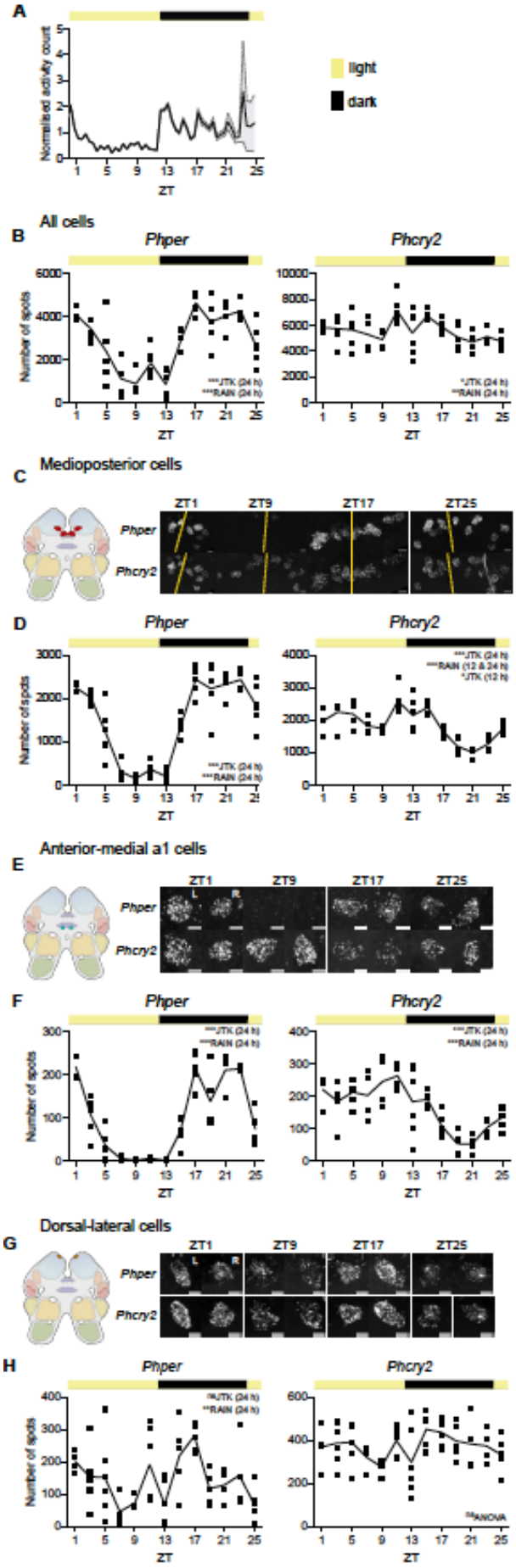
A
Normalised activity count
ZT
light
dark
All cells
B
Phper
Phcry2
Number of spots
ZT
Medioposterior cells
C
ZT1
ZT9
ZT17
ZT25
Phper
Phcry2
D
Phper
Phcry2
Number of spots
ZT
Anterior-medial a1 cells
E
ZT1
ZT9
ZT17
ZT25
L
R
Phper
Phcry2
F
Phper
Phcry2
Number of spots
ZT
Dorsal-lateral cells
G
ZT1
ZT9
ZT17
ZT25
L
R
Phper
Phcry2
H
Phper
Phcry2
Number of spots
ZT

Figure 6. Time course of expression of *per* and *cry2* in cells of *P. hawaiensis* synchronised to the LD cycle.

(A) Normalised swimming activity (mean +SEM, shading) of *P. hawaiensis* synchronised to the LD cycle and harvested for the HCR-FISH time-course (initial group size at start of harvest at ZT1 =79).

(B) Mean aggregate expression, quantified as the number of FISH spots, of *Phper* and *Phcry2* across all cells plotted across time in animals entrained to, and sampled under, a 12 h:12 h LD cycle. Each point is from one brain.

(C) Left: cartoon to show location of medioposterior cell group in the brain. Right: representative maximum intensity Z-projections of *Phper* and *Phcry2* expression in both hemispheres (L: left, R: right) across ZT (individual HCR-FISH channels in rows). Scale bars: 5 µm.

(D) Plots of mean transcript abundance, quantified as the number of FISH spots, across daily time for *Phper* (left) and *Phcry2* (right).

(E, F) as for C and D for anterior-medial 1a cells.

(G, H) as for C and D for dorsal-lateral cells.

Inset text in a and c indicate statistical tests (JTK-cycle and RAIN) performed to determine 24-hour rhythmicity. $p < 0.001$***, $p < 0.01$**, $p \leq 0.05$*, $p > 0.05^{ns}$. See also Supplementary Figure 14 for other cell groups with 24-h cycling in clock gene expression. For statistics and data shown in this figure, refer to Supplementary Table 6.

A Medioposterior cells

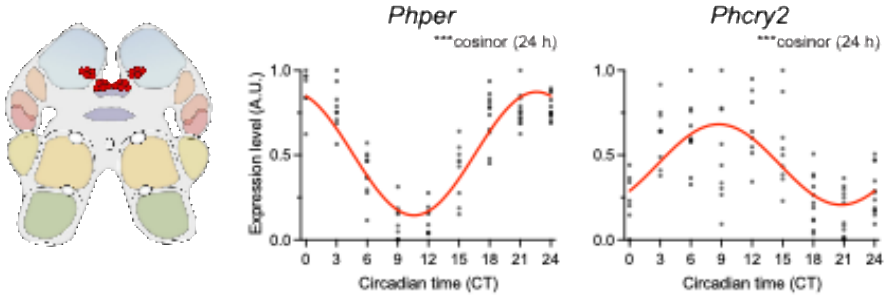

B Anterior-medial a1 cells

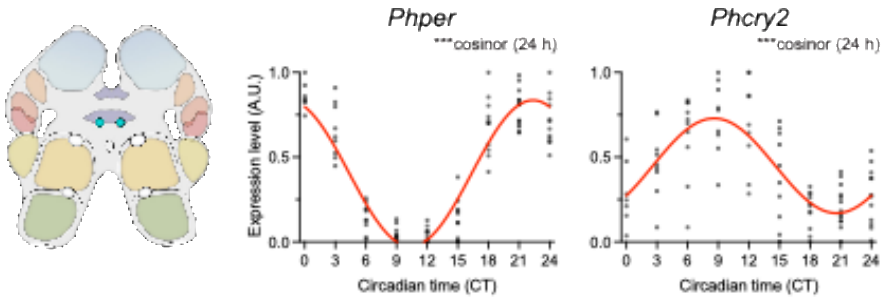

C Dorsal-lateral cells

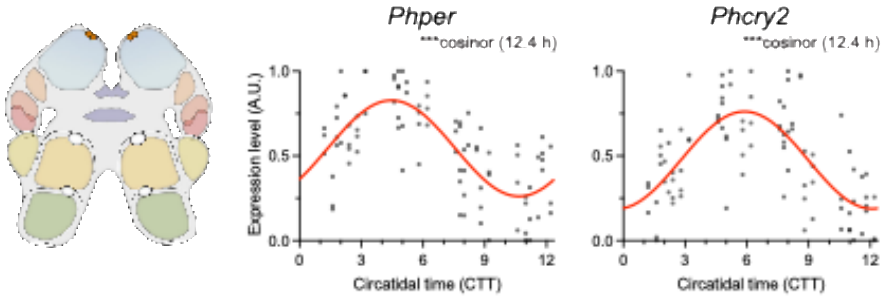

D Aligned to CT0

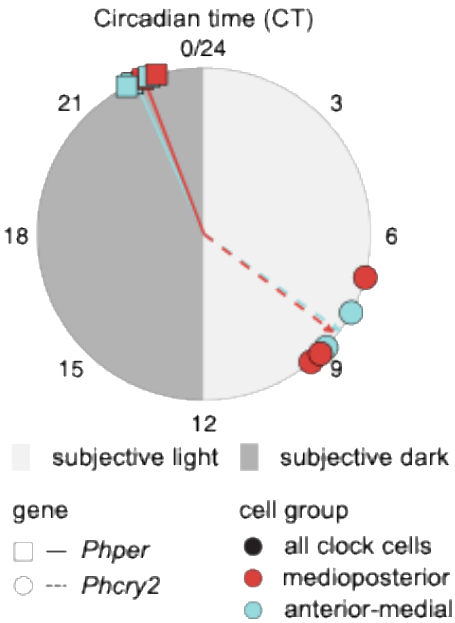

E Aligned to CTT0

Dorsal-lateral cells

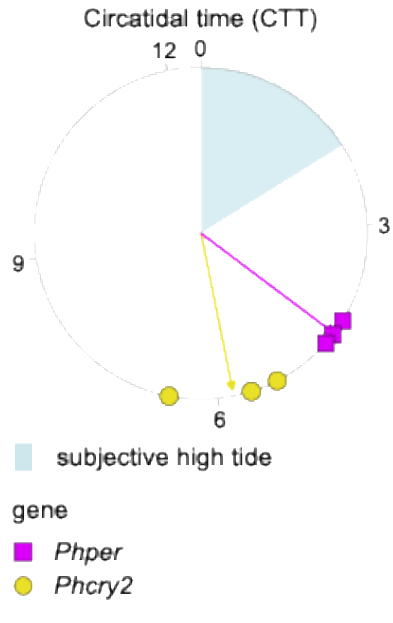

Figure 7. Summary meta-analysis of circatidal and circadian rhythms of clock gene expression in medioposterior, anterior-medial a1 and dorsal-lateral cell groups of *P. hawaiensis*.

(A) Left: cartoon to show location of the medioposterior cell group in the brain. Right: scatter plot of expression of *Phper* (left) and *Phcry2* (right) across three independent experiments registered to subjective circadian time (Circadian Time, CT =0). Red lines indicate 24-h cosinor fits.

(B) As in A for anterior-medial a 1cell group.

(C) As in A for dorsal-lateral cell group but plots are registered to subjective high tide (Circatidal Time, CTT =0). Red lines indicate 12.4-h cosinor fits.

Inset text in A-C indicate statistical significance of cosinor

(D) Circular plot of circadian peak expression phase of *Phper* and *Phcry2* in selected rhythmic cell groups of *P. hawaiensis* exhibiting circatidal activity rhythms. Each colour-shape combination represents data from across N =3 experiments. Arrowed lines indicate mean phase for each gene-cell group combination, and length of arrowed lines indicates mean resultant length of the vector at each mean.

(E) Circular plots of circatidal peak expression phase of *Phper* and *Phcry2* in the dorsal-lateral cells of *P. hawaiensis* exhibiting circatidal activity rhythms, with the circatidal acrophase aligned to CTT0 within each individual experiment. Arrowed lines indicate mean phase for each gene-cell group combination, and length of arrowed lines indicates mean resultant length of the vector at each mean. For mean phase and mean vector lengths for each gene-cell group combination in D and E, see Supplementary Table 7.

Supplementary materials: Figures, Tables, Results, Methods and References.

Supplementary Figures and Legends

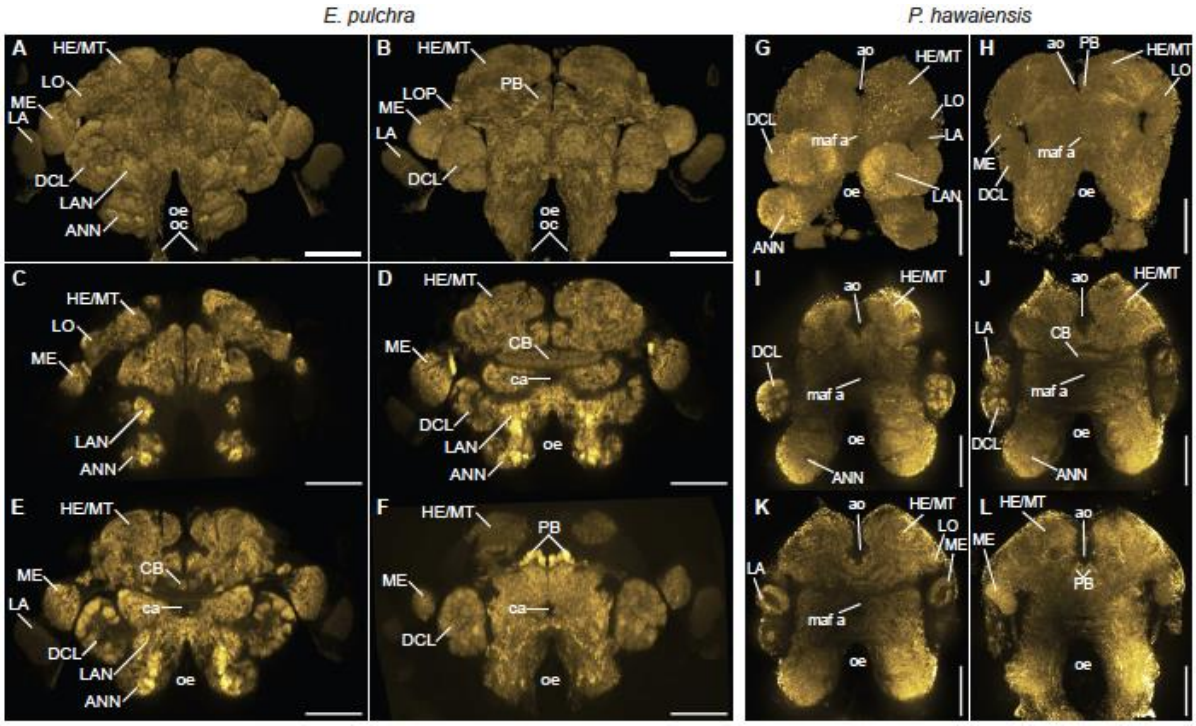

Supplementary Figure 1. Overview of representative *E. pulchra* and *P. hawaiensis* brains, immunostained with anti-SYNORF1 to highlight the neuropils.

(A) Anterior view of a *E. pulchra* brain (3D volume projection), with optic lobes, deutocerebral chemosensory lobes, antenna neuropils and hemi-ellipsoid body/medulla terminalis complexes are visible on the anterior surface of the brain.

(B) Posterior view of a *E. pulchra* brain (3D volume projection). The optic lobes, deutocerebral chemosensory lobes and hemi-ellipsoid body/medulla terminalis complexes are visible on the posterior surface. The protocerebral bridge appears as a distinct arch-like structure under the hemi-ellipsoid body/medulla terminalis complexes.

(C- E) Selected optical sections of a *E. pulchra* brain from anterior to posterior, showing locations of distinct neuropils throughout the depth of the brain. The optic lobes span the anterior-posterior axis, with the lobula constrained to the anterior aspect (C), and the medulla and lamina (D, E) occupying the medial and posterior aspects. The cigar-shaped central body is at its most expansive towards the middle of the brain.

(F) Maximum intensity Z-projection through the protocerebral bridge of a *E. pulchra* brain.

(G) Anterior view of a *P. hawaiensis* brain (3D volume projection), with parts of the optic lobes (lamina and lobula), deutocerebral chemosensory lobes, antenna neuropils and hemi-ellipsoid body/medulla terminalis complexes are visible on the anterior surface of the brain.
(H) Posterior view of a *P. hawaiensis* brain (3D volume projection). Parts of the optic lobes (medulla and lobula), deutocerebral chemosensory lobes and hemi-ellipsoid body/medulla terminalis complexes are visible on the posterior surface. As in *E. pulchra,* the protocerebral bridge of *P. hawaiensis* is located posteriorly under the hemi-ellipsoid body/medulla terminalis complexes.
(I- K) Selected optical sections of a *P. hawaiensis* brain from anterior to posterior, showing locations of distinct neuropils throughout the depth of the brain. The hemi-ellipsoid body/medulla terminalis complexes and the foramina accommodating two of the brain arteries, the anterior aorta and myoarterial formation a, are visible throughout the thickness of the brain. The former also constitute the most dorsal neuropils of the brain. The deutocerebral chemosensory lobes are located anterior to the rest of the optic lobes (I, J). The lamina is the most anteriorly positioned optic neuropils (J), followed almost simultaneously by the medulla and lobula (K). The sausage-shaped central body is at its most expansive towards the middle of the brain (J).
(I) Maximum intensity Z-projection through the protocerebral bridge of a *P. hawaiensis* brain.
Abbreviations: ANN, antenna 2 neuropil; ao, anterior aorta; ca, cerebral artery; CB, central body; DCL, deutocerebral chemosensory lobe; HE/MT, hemi-ellipsoid body/medulla terminalis; LA, lamina; LAN, lateral antenna 1 neuropil; LO, lobula; LOP, lobula plate; maf a, myoarterial formation a; ME, medulla; oc, oesophageal connective; oe, oesophageal foramen; PB, protocerebral bridge. Scale bars*:* 100 μm.

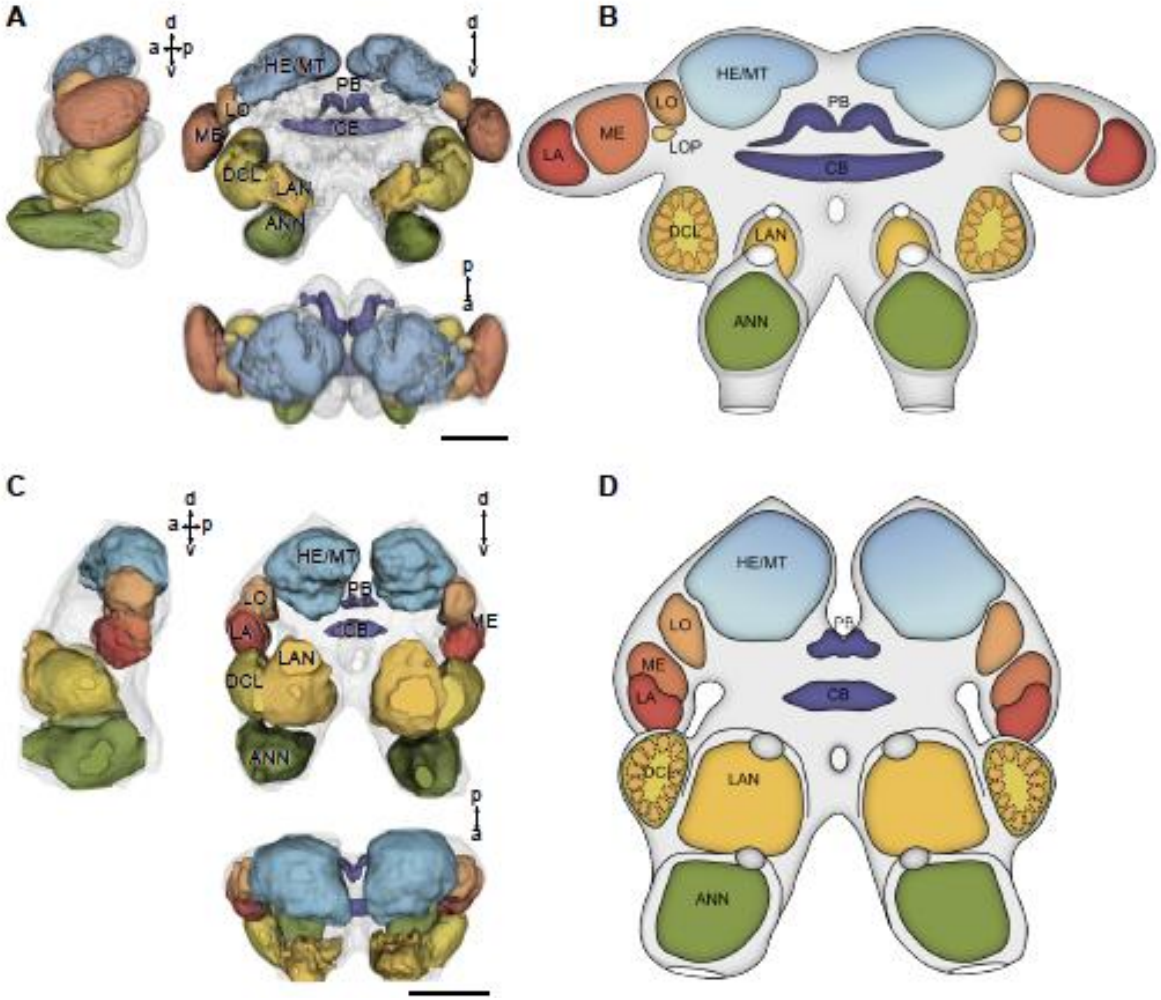

Supplementary Figure 2. Gross anatomy of *E. pulchra* and *P. hawaiensis* brains revealed by anti-SYNORF1 immunostaining, registered to refence brain.

(A) Lateral, anterior and dorsal views of the *E. pulchra* surface-rendered 3D average reference brain, with major neuropils demarcated. See also Supplementary Video 1.

(B) Diagrammatic representation of the of *E. pulchra* brain, based on A.

(C) Lateral, anterior and dorsal views of *P. hawaiensis* surface-rendered 3D average reference brain with major neuropils demarcated. See also Supplementary Video 2.

(D) Diagrammatic representation of the *P. hawaiensis* brain, based on C.

Compass markers in A and C show anterior (a), posterior (p), dorsal (d) and ventral (v) directions.

Abbreviations: ANN antenna 2 neuropil, CB central body, DCL deutocerebral chemosensory lobe, HE/MT medulla terminalis/ hemi-ellipsoid body, LA lamina, LAL lateral accessory lobe, LAN lateral antenna 1 neuropil, LO lobula, LOP lobula plate, ME medulla, PB protocerebral bridge. Scale bars: 100 µm.

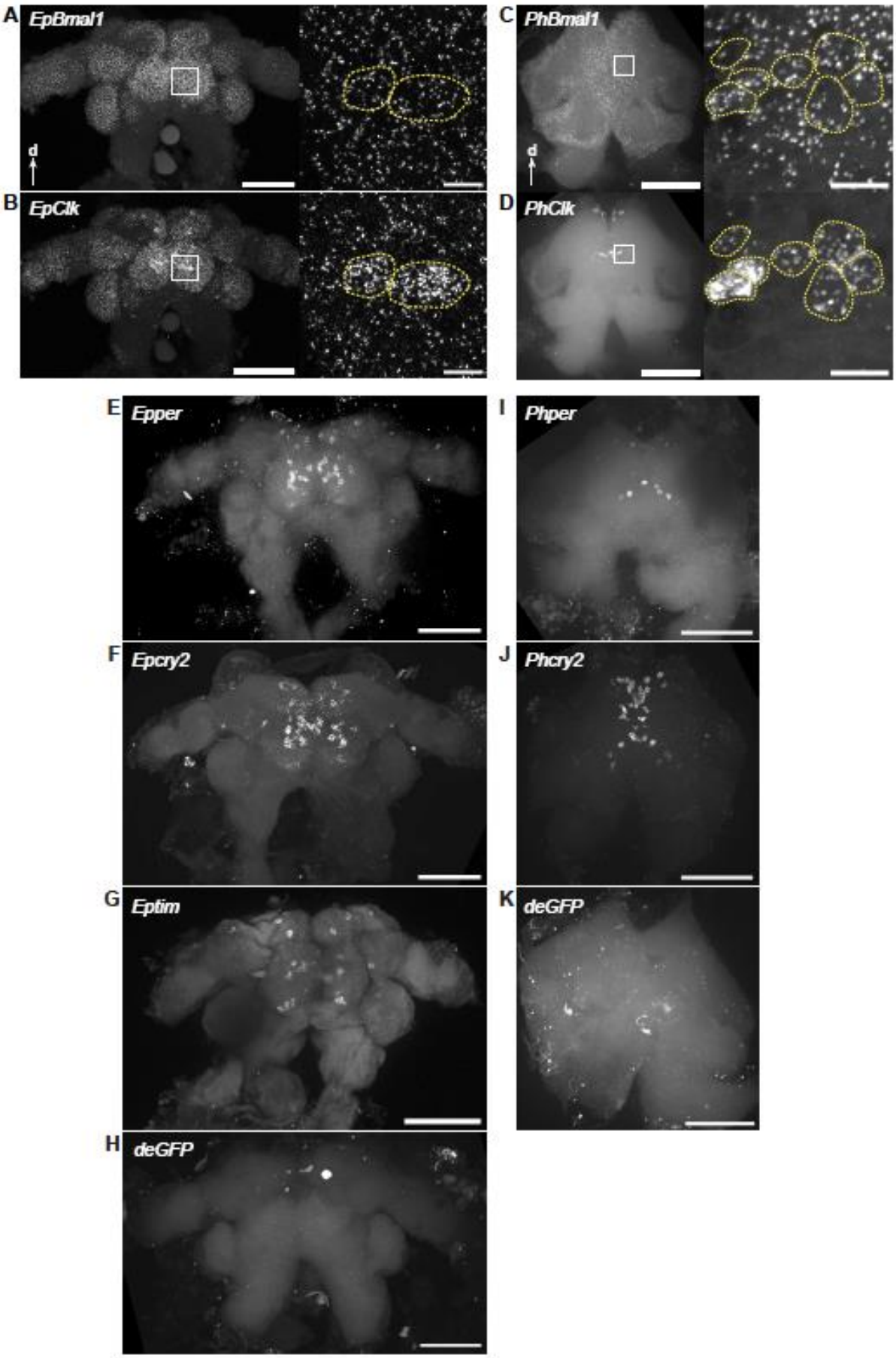
A
EpBmal1
d
B
EpClk
C
PhBmal1
d
D
PhClk
E
Epper
F
Epcry2
G
Eptim
H
deGFP
I
Phper
J
Phcry2
K
deGFP

Supplementary Figure 3. Expression of circadian clock positive and negative regulators across the brains of *E. pulchra* and *P. hawaiensis*.

(A) Left panel: maximum intensity Z-projection of image stack of an entire *E. pulchra* brain (posterior apposing coverslip) probed for circadian factor *EpBmal1* using HCR-FISH. Right panel: maximum intensity Z-projection of two-cell-thick image stack (16 µm) from the boxed region of the brain in the left panel.

(B) As in A, probed for circadian factor, *EpClk*.

(C) Left panel: maximum intensity Z-projection of image stacks of a *P. hawaiensis* brain (anterior apposing coverslip) probed for circadian factor *PhBmal1*. Right panel: maximum intensity Z-projection of two-cell-thick image stacks (24 µm) from the boxed region of the brain in the left panels.

(D) As in C, probed for circadian factor, *PhClk*.

(E, F, G, H) Maximum intensity Z-projections of image stacks of *E. pulchra* brains (posterior apposing coverslip) probed for circadian clock repressors, *Epcry2, Epper*, *Eptim* and the negative control probe *deGFP* HCR-FISH.

(I, J, K) Maximum intensity Z-projections of image stacks of *P. hawaiensis* brains (anterior apposing coverslip) probed for circadian clock repressors, *Phcry2*, *Phper* and the negative control probe *deGFP*. Scale bars: 100 µm.

Arrows indicate dorsal orientation. Yellow dotted outlines in A- D indicate cells in which *Clk* expression is enriched. Scale bars: 100 µm (A-D: left panels, E-K) and 10 µm (A-D: right panels).

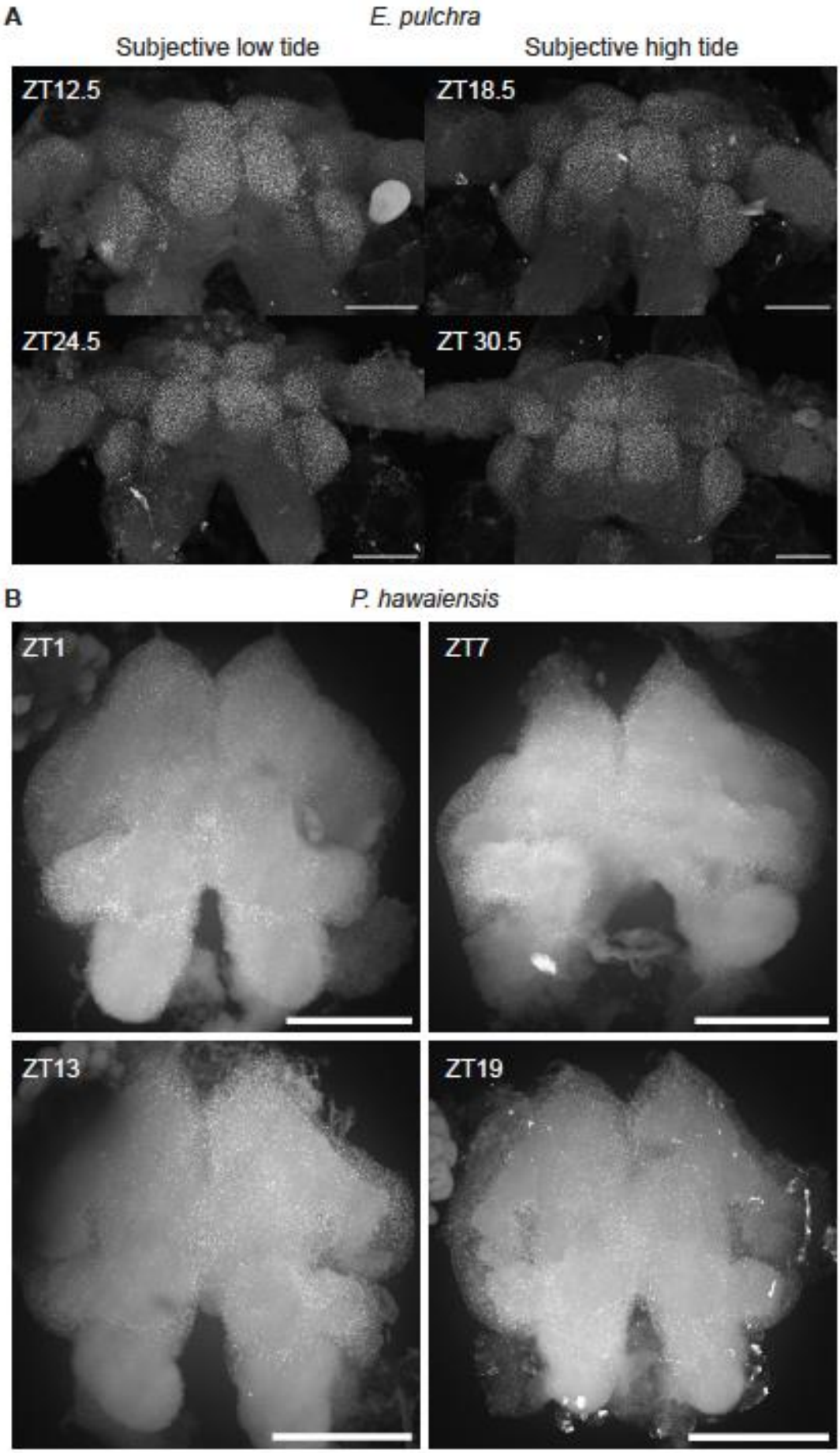
A
E. pulchra
Subjective low tide
Subjective high tide
ZT12.5
ZT18.5
ZT24.5
ZT 30.5
B
P. hawaiensis
ZT1
ZT7
ZT13
ZT19

Supplementary Figure 4. Cellular expression of *Bmal1* in brains of *E. pulchra* and *P. hawaiensis* across time.

(A) Maximum intensity Z-projections of representative brains (posterior apposing coverslip) from field-collected *E. pulchra* sampled under 14 h: 10 h LD cycle and then probed for *EpBmal1* using HCR-FISH.

(B) Maximum intensity Z-projections of representative *P. hawaiensis* brains (anterior apposing coverslip) sampled under 12 h: 12 h LD cycle and then probed for *PhBmal1* using HCR-FISH. Scale bars: 100 μm.

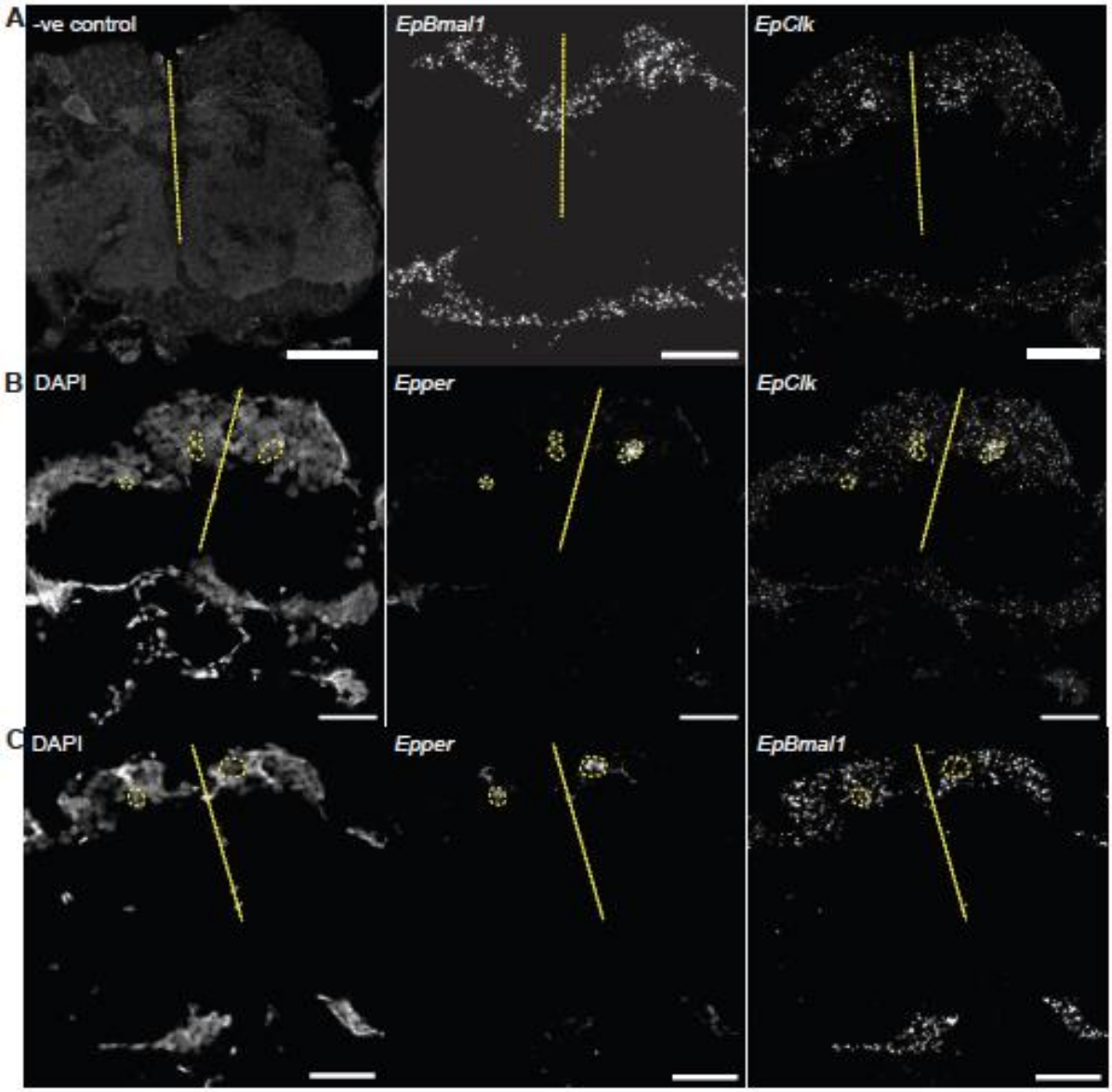

Supplementary Figure 5. Expression of circadian clock genes in *E. pulchra* brain sections detected using RNAScope™.

(A) Representative image (single optical section) of *E. pulchra* brain sections probed for negative control (left), *EpBmal1* (middle) and *EpClk* (right).

(B) Representative image (single optical section) of a *E. pulchra* brain section stained with DAPI (left) and probed for *Epper* (middle) and *EpClk* (right).

(C) As in B for *Epper* and *EpBmal1*.

Yellow dashed outlines indicate cells enriched for *Epper* and *EpClk* expression. Yellow dotted lines indicate midlines. Scale bars: 10 µm.

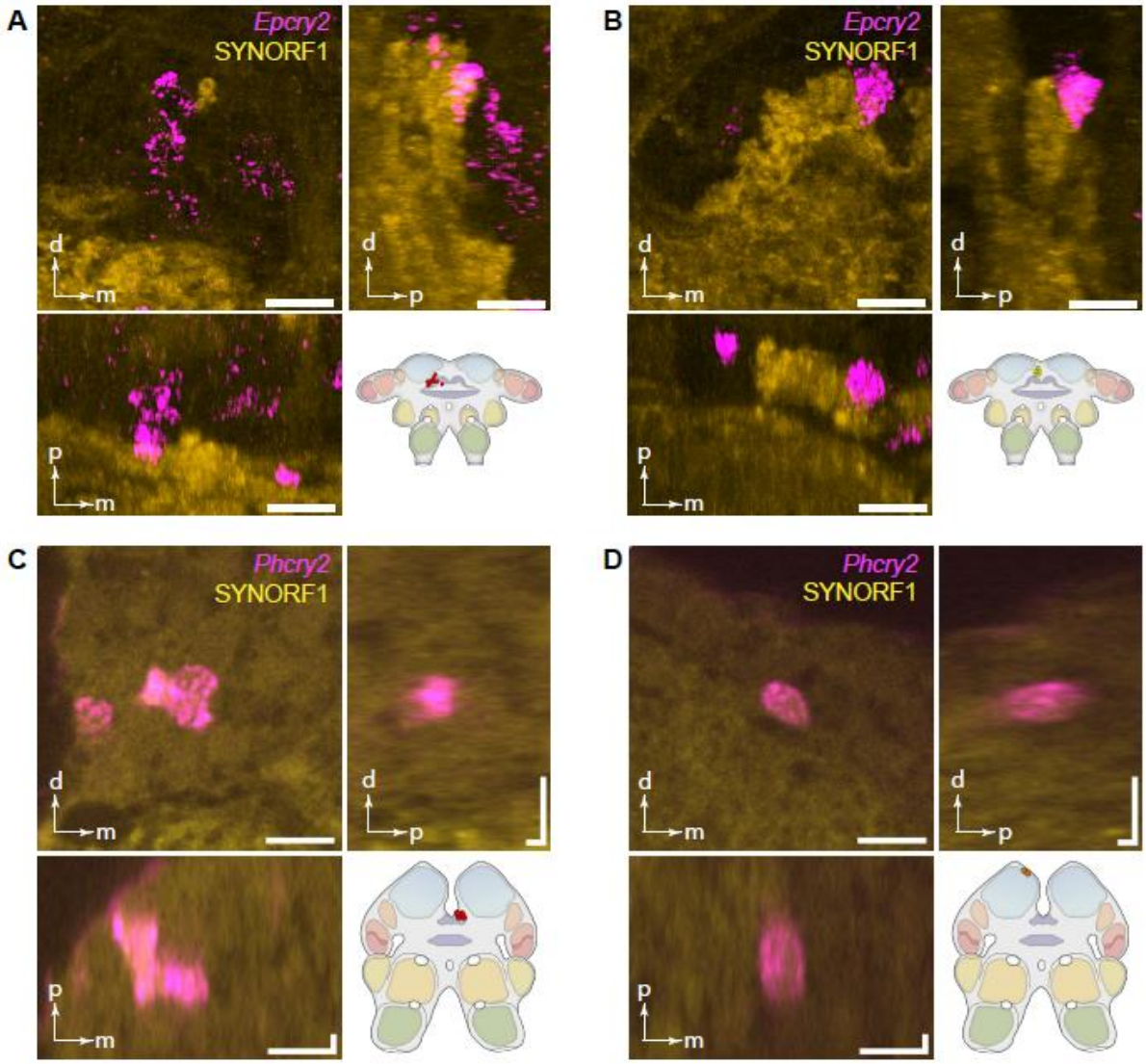

Supplementary Figure 6. Representative orthogonal views of brains co-labelled with anti-SYNORF1 (IHC) and *cry2* (HCR-FISH).

(A) Orthogonal views showing *Phcry2* enrichment in four medioposterior cells of a *E. pulchra* brain co-stained with anti-SYNORF1. Cartoon shows location of these cells.

(B) As in A but for the medial cells.

(C) Orthogonal views showing *Phcry2* enrichment in four medioposterior cells of a *P. hawaiensis* brain co-stained with anti-SYNORF1. Cartoon shows location of these cells.

(D) As in C but for the two dorsal-lateral cells.

Horizonal (and vertical) scale bars: 10 μm. Orientations: d: dorsal; p: posterior; m: medial.

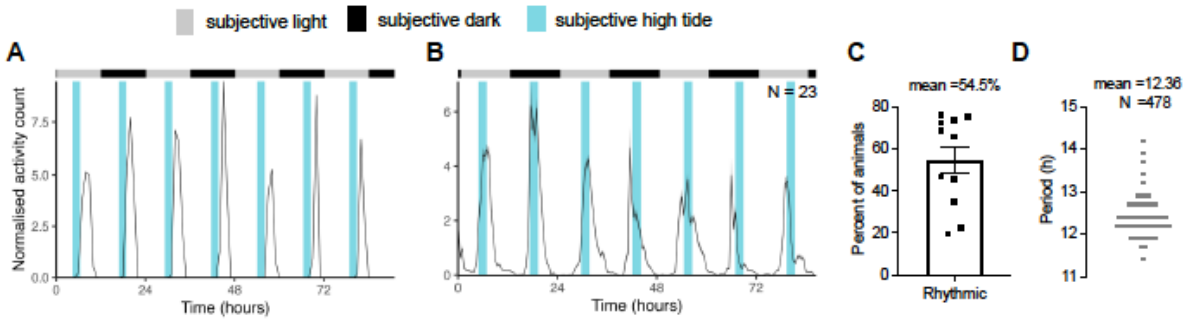

Supplementary Figure 7. Circatidal swimming behaviour of beach-collected *Eurydice pulchra* recorded in free-running laboratory conditions.

(A) Normalised swimming activity of a representative individual *E. pulchra*. Blue shadings indicate subjective high tides on home beach.

(B) Mean normalised swimming activity profile for a group of animals under DD from the same experiment as the individual in A (N =23).

(C) Percentage of animals showing rhythmic swimming behaviour from 11 independent experiments, representing 11 beach collections from 2022 to 2024. Error bars indicate SEM.

(D) Individual periods of beach-caught *E. pulchra* swimming activity under DD across all experiments. Mean (±SEM) is 12.36 ±0.02 h (N =478).

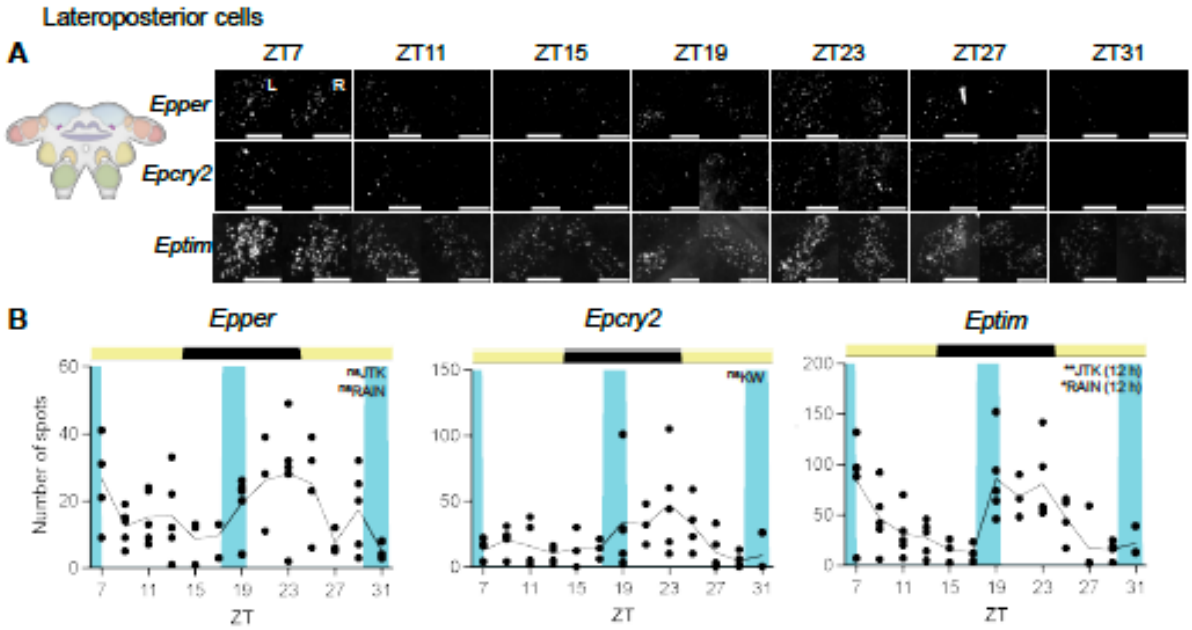

Supplementary Figure 8. Time course of expression of *per, cry2* and *tim* in lateroposterior cells of tidally rhythmic *E. pulchra* held on a LD cycle.

(A) Left: Cartoon to show location of lateroposterior cell group in the brain and Right: representative maximum intensity Z-projections of *Epper*, *Epcry2* and *Eptim* expression in lateroposterior cells in both hemispheres (L: left, R: right) across ZT (individual HCR-FISH channels in rows).

(B) Plots of mean transcript abundance, quantified as the number of FISH spots, across ZT for *Epper* (left), *Epcry2* (middle) and *Eptim* n (right) in the lateroposterior cells. Each point is from one brain.

Inset text indicates statistical tests performed to determine variation of gene expression with time and/or rhythmicity, with the tested periods (if any) in parentheses. p <0.001***, p <0.01**, p ≤0.05*, p >0.05^{ns}. For statistics shown in this figure, refer to Supplementary Table 2. Scale bars: 10 µm (A, C).

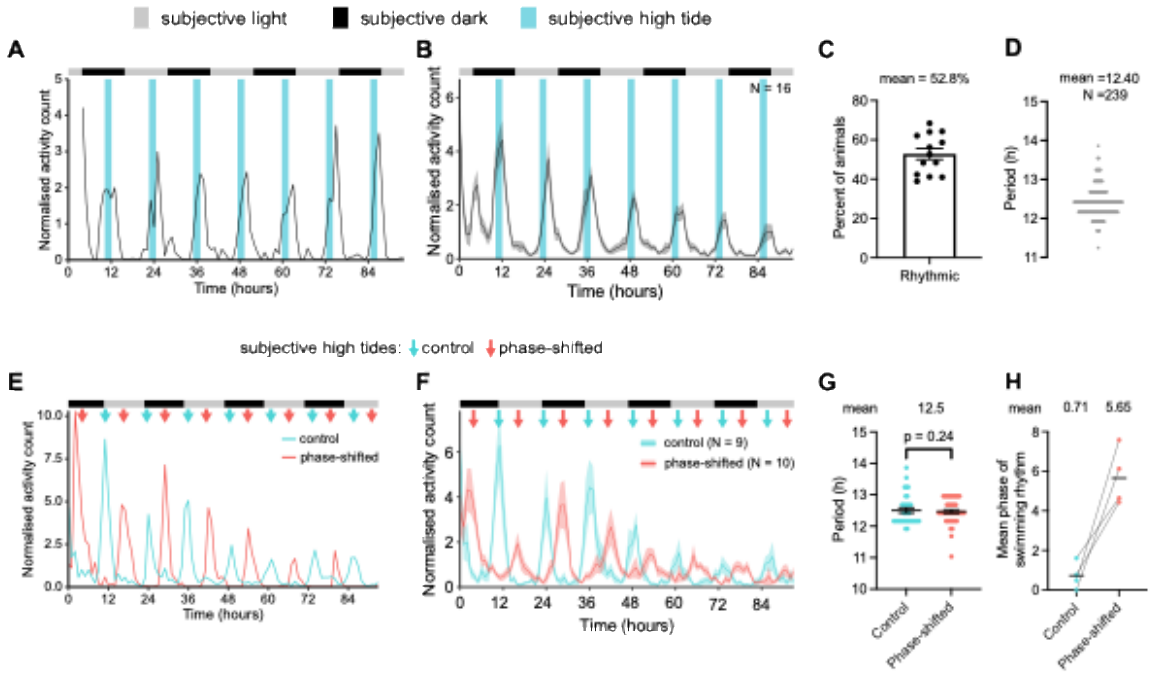

Supplementary Figure 9. Laboratory-cultured *P. hawaiensis* show circatidal activity rhythms after entrainment to a tidal cycle of 2 hours of mechanical agitation every 12.4 hours simulating high water.

(A) Normalised swimming activity of individual laboratory-cultured *P. hawaiensis* free-running under DD (grey/ black bars), following entrainment to 2 h of agitation every 12.4 h. Blue bars indicate time of subjective tidal agitation.

(B) Mean normalised swimming activity profile for all circatidal rhythmic *P. hawaiensis* under DD (grey/ black bars) from the same experiment as the individual in A (N =16). Blue bars indicate time of subjective tidal agitation, shaded area indicates ±SEM.

(C) Percentage of animals showing a circatidal rhythm in swimming activity after tidal entrainment by agitation. Data from 13 independent experiments (N =456). Error bars indicate SEM.

(D) Individual periods of circatidal locomotor activity under DD of tidally entrained *P. hawaiensis.* Mean (±SEM) is 12.40 ±0.02 h (N =239).

(E) Representative activity recording of two individual laboratory-cultured *P. hawaiensis* free-running under DD (black/ grey bars) following prior tidal entrainment at a period of 12.4 h (cyan, control) or 12.9 h (red, phase-shifted) over 6 days. Arrows indicate times of subjective tidal agitation for the control and phase-shifted animals.

(F) Mean normalised swimming activity profile for all circatidally rhythmic *P. hawaiensis* under DD (grey/ black bars) from the same experiment as the individuals in E ($N_{control}$ =9, $N_{phase\text{-}shifted}$

=10). Arrows indicate times of subjective tidal agitation for the control and phase-shifted groups, shaded area indicates ±SEM.

(G). Individual periods of circatidal activity rhythm of *P. hawaiensis* after tidal entrainment by agitation under control and phase-shifted conditions (4 independent experiments, $N_{control}$ =34, $N_{phase\text{-}shifted}$ =42, Kolmogorov-Smirnov test: D =0.24, p =0.24, n.s.). Horizontal lines indicate mean phase within each group, and error bars indicate SEM.

(H) Mean phase of circatidal activity rhythms of paired control and phase-shifted groups across 4 replicate experiments as in F. The subjective high tide onset of the earliest control group defined phase =0. Horizontal lines indicate mean phase within each group.

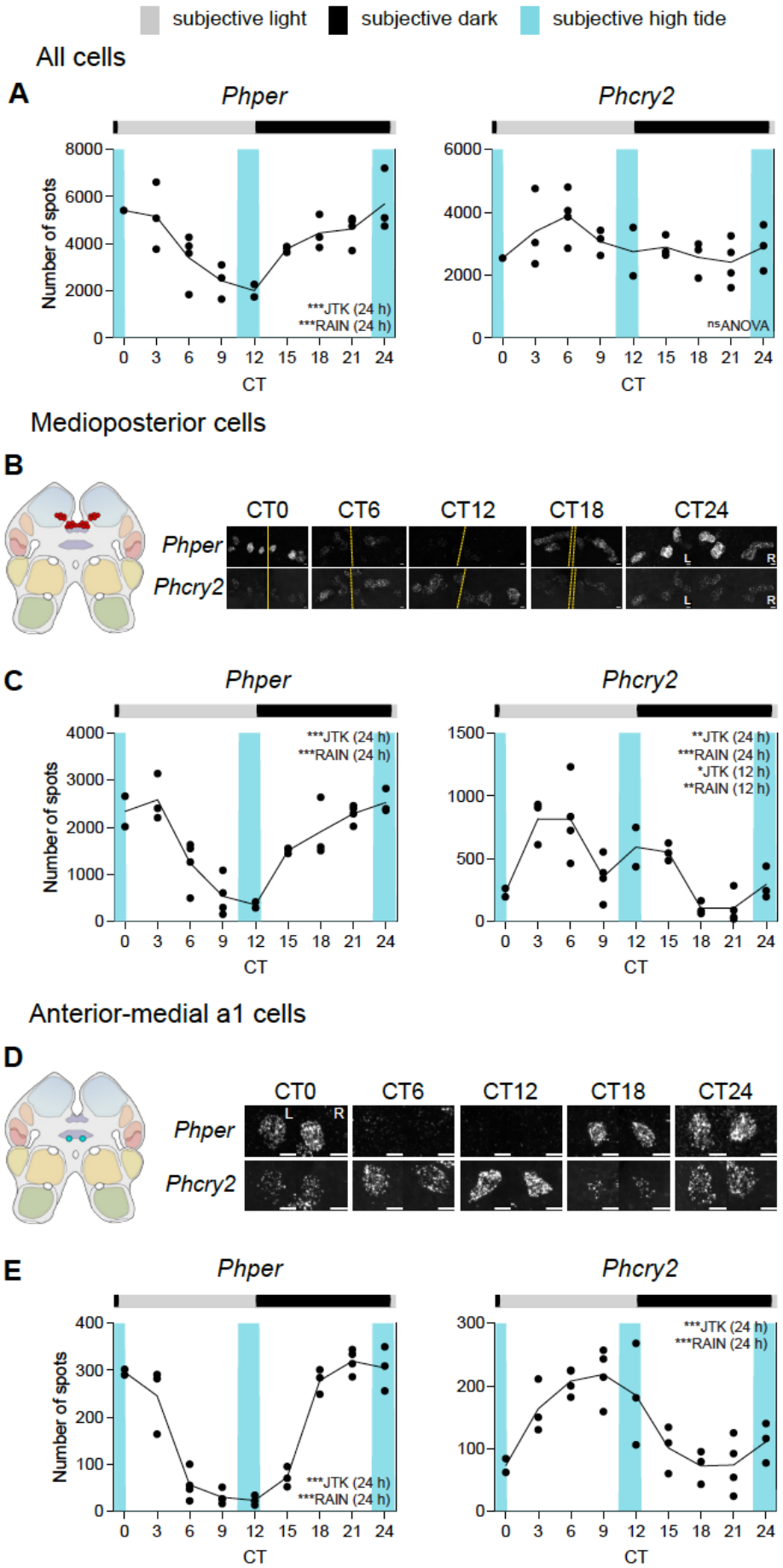
subjective light
subjective dark
subjective high tide
All cells
A
Phper
Phcry2
Number of spots
***JTK (24 h)
***RAIN (24 h)
nsANOVA
CT
Medioposterior cells
B
CT0
CT6
CT12
CT18
CT24
Phper
Phcry2
L
R
C
Phper
Phcry2
Number of spots
***JTK (24 h)
***RAIN (24 h)
**JTK (24 h)
***RAIN (24 h)
*JTK (12 h)
**RAIN (12 h)
CT
Anterior-medial a1 cells
D
CT0
CT6
CT12
CT18
CT24
Phper
Phcry2
L
R
E
Phper
Phcry2
Number of spots
***JTK (24 h)
***RAIN (24 h)
CT

Supplementary Figure 10. Free-running clock gene expression rhythms in tidally entrained *P. hawaiensis* (tidal phase θ + 1.2 h).

(A) Mean aggregate expression, quantified as the number of FISH spots, of Phper and *Phcry2* across all cells plotted across time in tidally entrained animals sampled under DD. Each point is from one brain.

(B) Left: Cartoon to show location of medioposterior cell group in the brain and Right: representative maximum intensity Z-projections of *Phper* and *Phcry2* expression in the medioposterior cells from both hemispheres (L: left, R: right, yellow dashed lines: midlines) across CT (individual HCR-FISH channels in rows).

(C) Mean transcript abundance, quantified as the number of FISH spots, across CT for *Phper* (left) and *Phcry2* (right)) in the medioposterior cells. Each point is from one brain.

(D, E) As in B, C for anterior-medial a1 cell group.

Inset text indicates statistical tests performed to determine variation of gene expression with time and/or rhythmicity, with the tested periods (if any) in parentheses. $p < 0.001$***, $p < 0.01$**, $p \leq 0.05$*, $p > 0.05^{ns}$. KW: Kruskal-Wallis test. For statistics shown in this figure, refer to Supplementary Table 4. Scale bars: 5 μm (B), 10 μm (D).

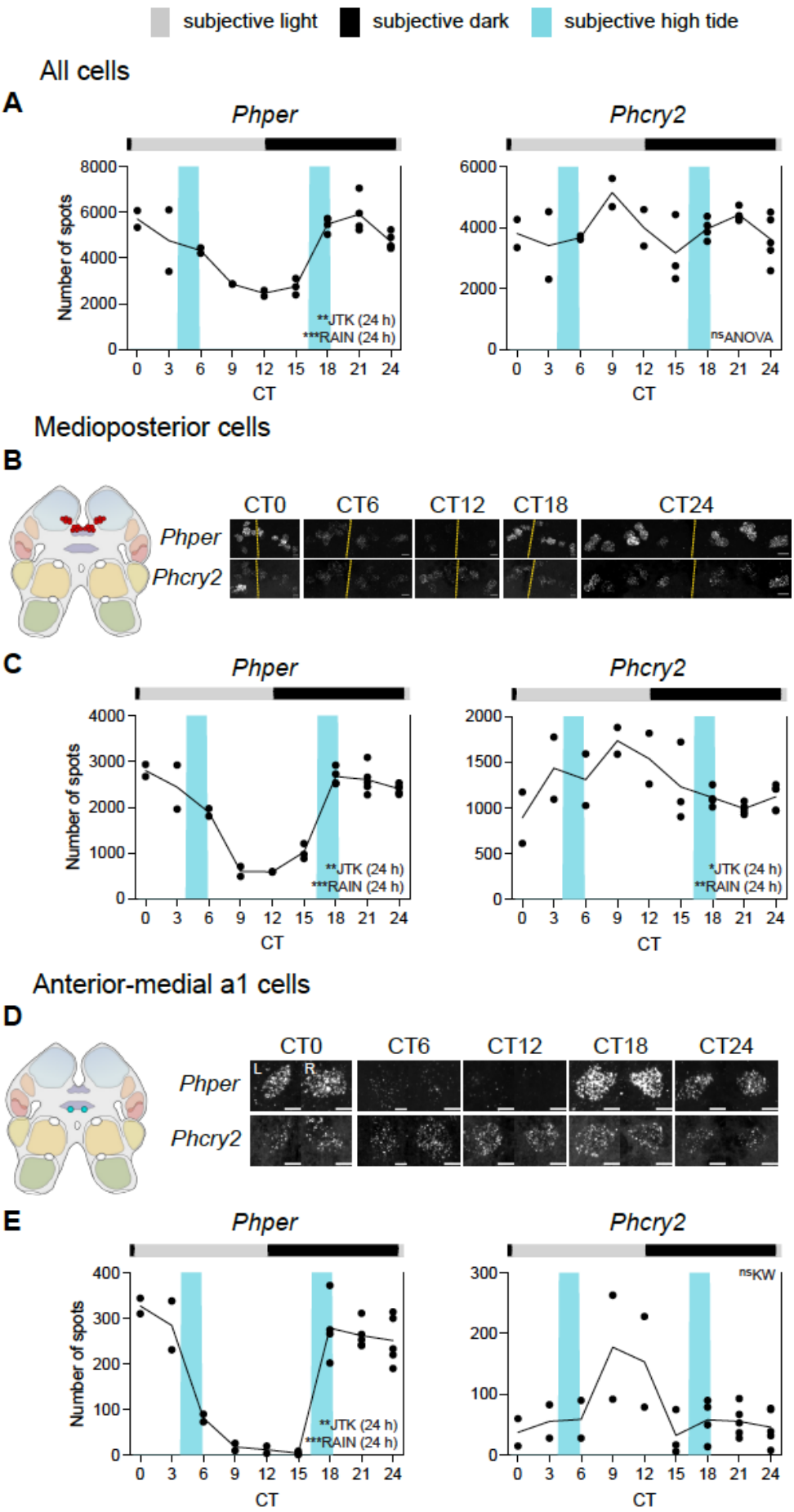
subjective light
subjective dark
subjective high tide
All cells
A
Phper
Phcry2
Number of spots
**JTK (24 h)
***RAIN (24 h)
nsANOVA
CT
Medioposterior cells
B
CT0
CT6
CT12
CT18
CT24
Phper
Phcry2
C
Phper
Phcry2
Number of spots
**JTK (24 h)
***RAIN (24 h)
*JTK (24 h)
**RAIN (24 h)
CT
Anterior-medial a1 cells
D
CT0
CT6
CT12
CT18
CT24
L
R
Phper
Phcry2
E
Phper
Phcry2
Number of spots
**JTK (24 h)
***RAIN (24 h)
nsKW
CT

Supplementary Figure 11. Free-running clock gene expression rhythms in tidally entrained *P. hawaiensis* (tidal phase θ +5.4 h).

(A) Mean aggregate expression, quantified as the number of FISH spots, of *Phper* and *Phcry2* across all cells plotted across time in tidally entrained animals sampled under DD. Each point is from one brain.

(B) Left: Cartoon to show location of medioposterior cells in the brain and Right: representative maximum intensity Z-projections of *Phper* and *Phcry2* expression in the anterior-medial a1 cells from both hemispheres (L: left, R: right, yellow dashed lines: midlines) across CT (individual HCR-FISH channels in rows).

(C) Mean expression, quantified as the number of FISH spots, across CT for *Phper* (left) and *Phcry2* (right) in the anterior-medial a1 cells. Each point is from one brain.

(D, E) As in B, C for anterior-medial a1 cell group.

Inset text indicates statistical tests performed to determine variation of gene expression with time and/or rhythmicity, with the tested periods (if any) in parentheses. $p < 0.001$***, $p < 0.01$**, $p \leq 0.05$*, $p > 0.05^{ns}$. KW: Kruskal-Wallis test. For statistics shown in this figure, refer to Supplementary Table 5. Scale bars: 5 μm (B), 10 μm (D).

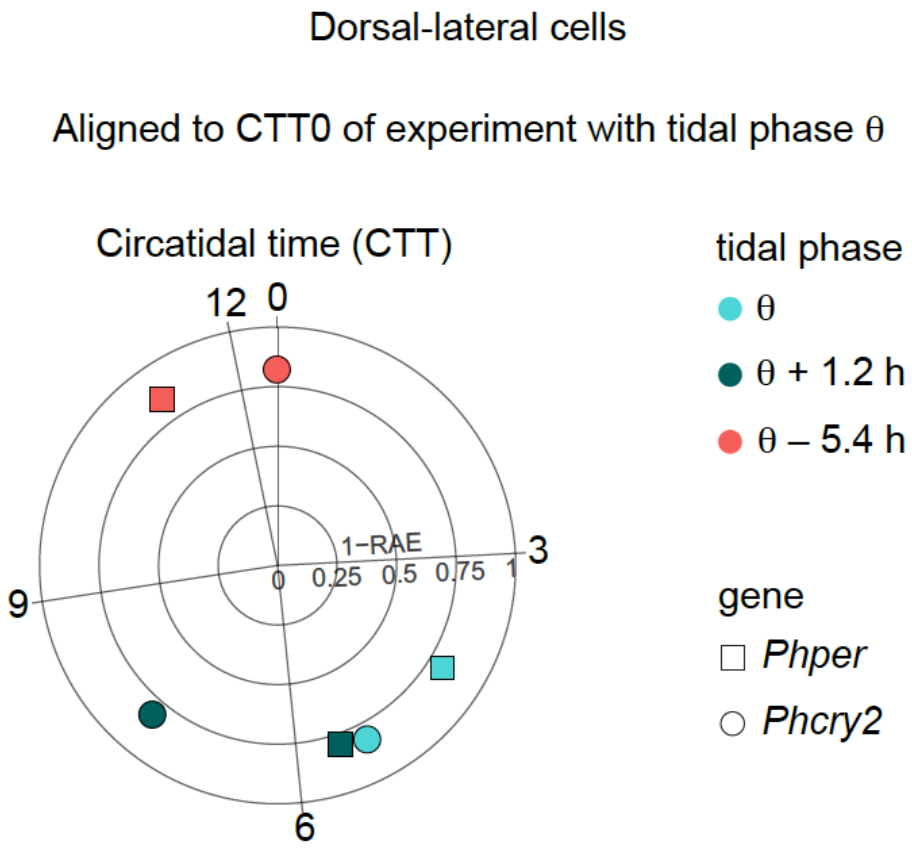

Supplementary Figure 12. Acrophase of free-running clock gene expression pattern in the dorsal lateral cells of *P. hawaiensis* entrained to tidal cycles of different phase. Circular plots of phase of circatidal peak expression of *Phper* and *Phcry2* in the dorsal-lateral cells of *P. hawaiensis* exhibiting circatidal activity rhythms. The phase of each experiment is aligned to circatidal time (CTT) =0 of the experiment with tidal phase θ. Each colour represents an individual experiment at each of different phases (total N =3 X 3). RAE: relative amplitude error.

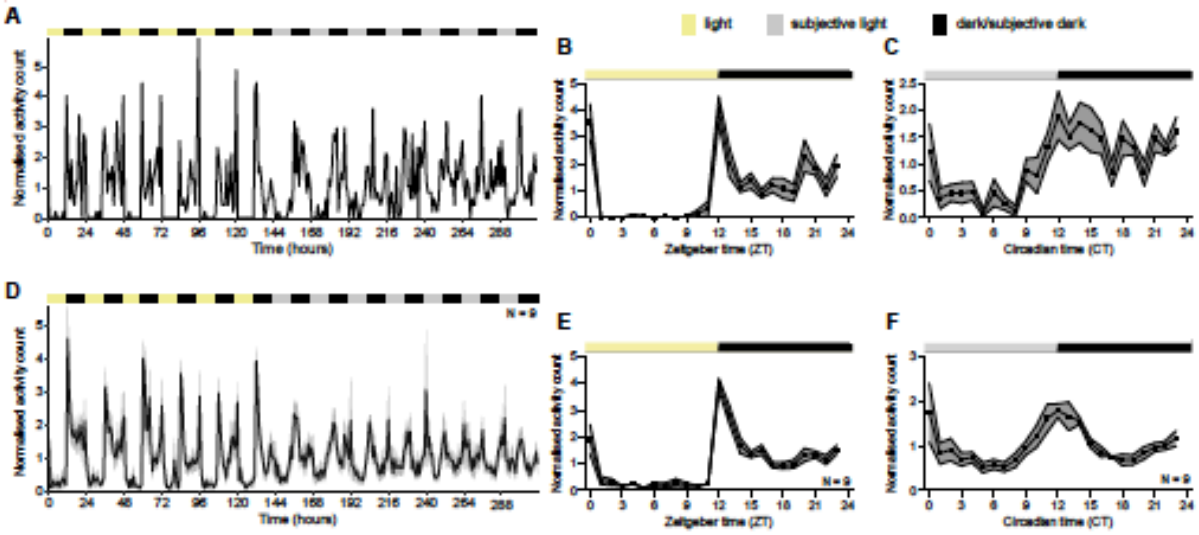

Supplementary Figure 13. Laboratory-cultured *P. hawaiensis* show circadian activity rhythms after entrainment to LD cycle.

(A) Representative activity recording of individual laboratory-cultured *P. hawaiensis*, which had never been subjected to tidal entrainment, initially maintained under 12 h:12 h L:D cycle (yellow/black bars) and then allowed to free-run under DD (grey/ black bars).

(B) Mean activity profile for the individual from A under LD showing higher activity during night-time. Shaded area indicates ±SEM.

(C) Mean activity profile for the individual from A under DD showing higher activity during subjective night. Shaded area indicates ±SEM.

(D, E and F) as for A, B and C but showing group data as mean ±SEM (shading, N =9).

Dorsal cells

A

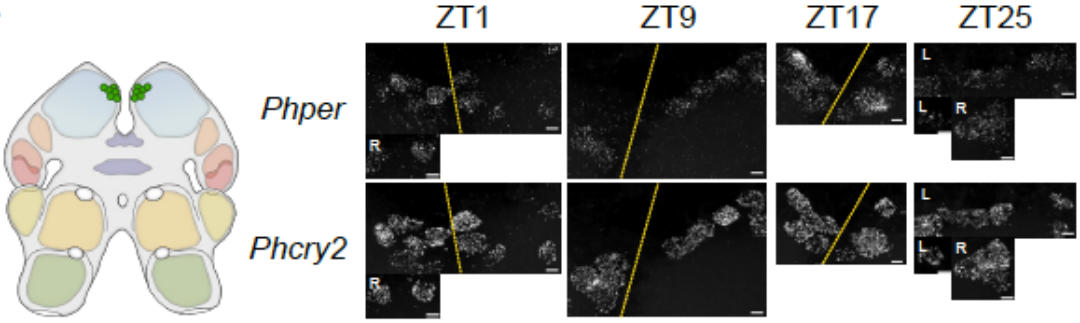

B

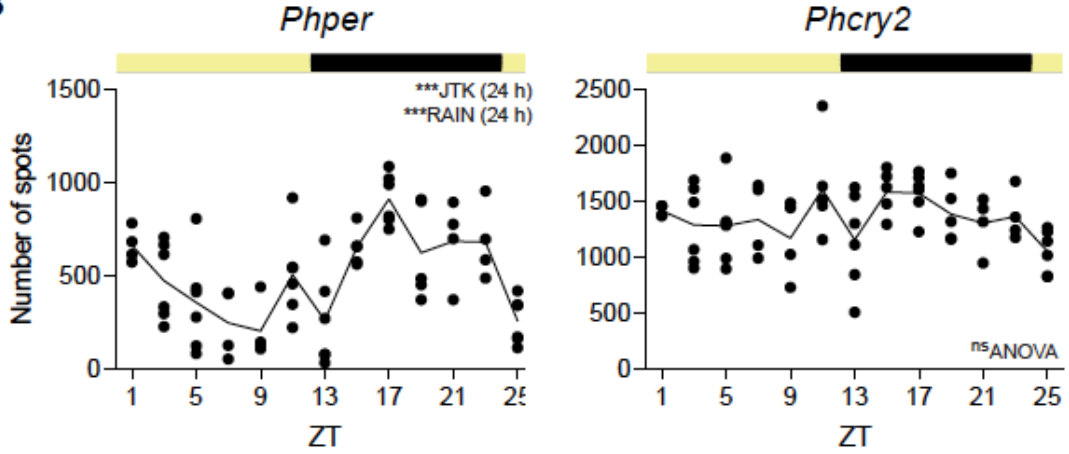

Anterior-medial b cells

C

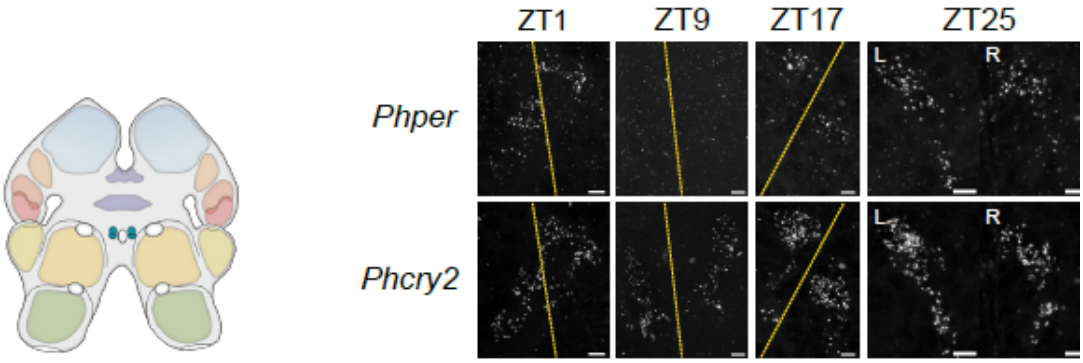

D

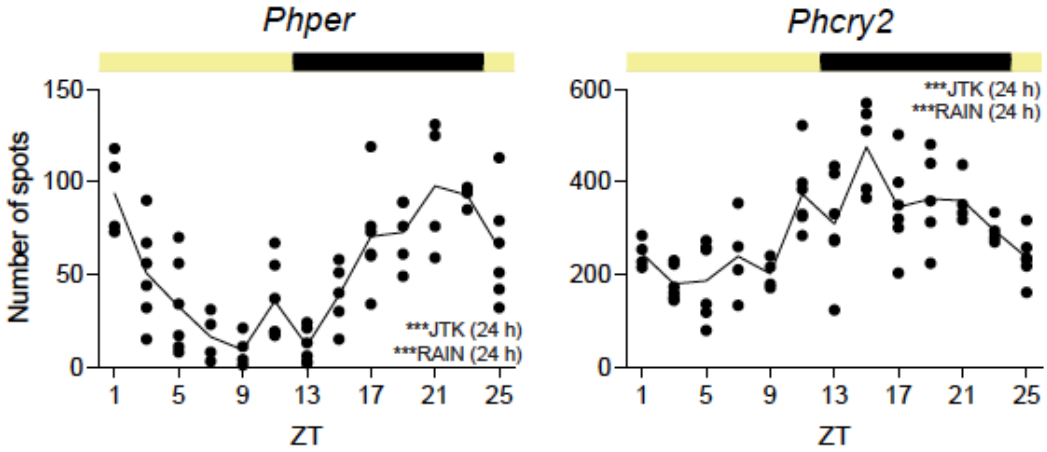

Supplementary Figure 14. Time course of rhythmic expression of *per* and *cry2* in cells of *P. hawaiensis* synchronised to the LD cycle.

(A) Left: Cartoon to show location of medioposterior cell group in the brain and Right: representative maximum intensity Z-projections of *Phper* and *Phcry2* expression in the medioposterior cells of both hemispheres (L: left, R: right, yellow dashed lines: midlines) across ZT (individual HCR-FISH channels in rows).

(B) Mean expression, quantified as the number of FISH spots, of *Phper* (left) and *Phcry2* in the dorsal cells plotted across daily time. Each point is from one brain.

(C, D) as in A, B for anterior-medial b cell group.

Inset text indicate statistical tests performed to determine variation of gene expression with time and/or rhythmicity, with the tested periods (if any) in parentheses. $p < 0.001^{***}$, $p < 0.01^{**}$, $p \leq 0.05^{*}$, $p > 0.05^{ns}$. Scale bars: 10 µm (b), 5 µm (d, f, h). For statistics shown in this figure, refer to Supplementary Table 6.

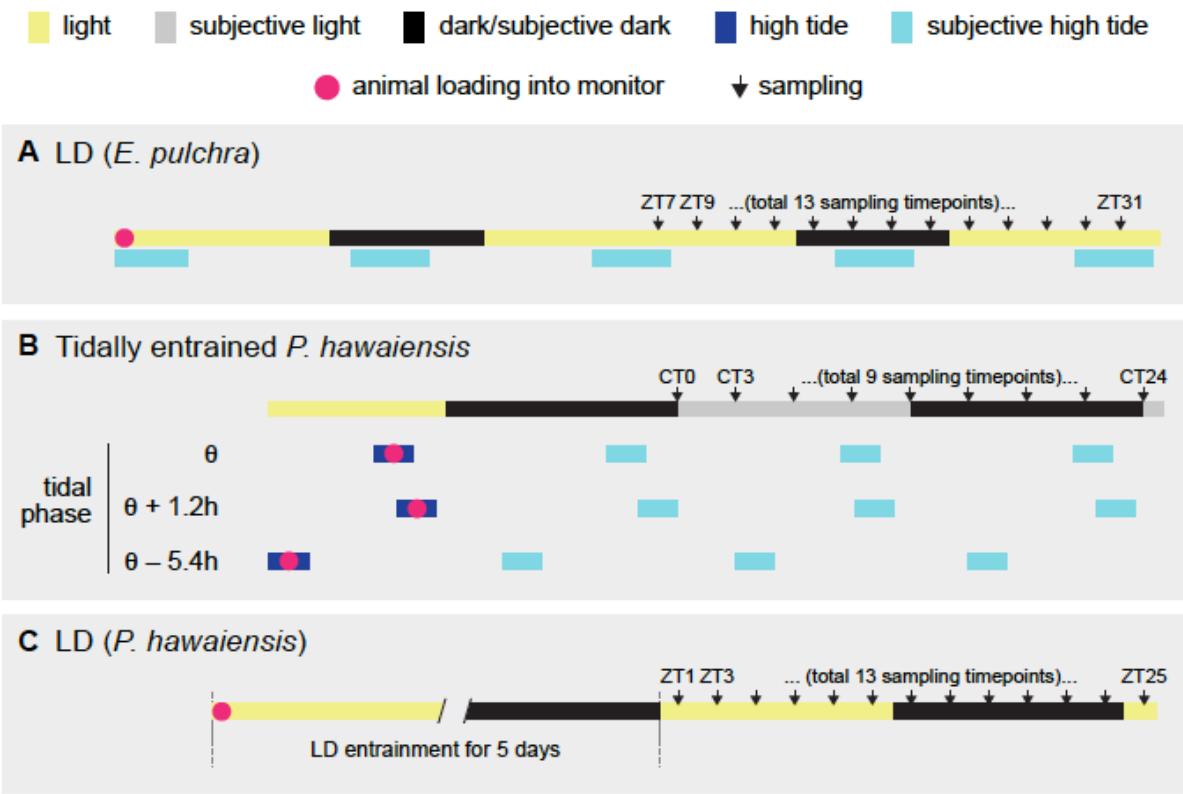

Supplementary Figure 15. HCR-FISH time-course design.

(A) Field-collected *E. pulchra* were loaded into activity monitors and maintained under 16 h: 8 h LD cycles. At ZT7 on the day after loading, animals showing circatidal rhythmicity in their swimming activity were sampled every 2 hours, for a total of 13 timepoints.

(B) Laboratory-cultured *P. hawaiensis* which had been subjected to tidal cycles of mechanical agitations were loaded into activity monitors whilst being shaken. At CT0 on the day after loading, animals showing peaks in activity coinciding with the subjective high tide during the night before were sampled every 3 hours, for a total of 9 timepoints.

Time-course design is also described in Supplementary Table 10.

(C) Laboratory-cultured *P. hawaiensis* that had never been tidally entrained were loaded into activity monitors and maintained under 12 h: 12 h LD cycles for 5 days. Animals showing 24-h rhythmicity over the 5-day LD entrainment period were sampled every 2 hours beginning at ZT1 on day 6, for a total of 13 timepoints.

Time-course design is also described in Supplementary Table 10.

Supplementary Table 1. Summary of cell groups enriched for *per* and *cry* expression in *E. pulchra* and *P. hawaiensis*.

E. pulchra				***P. hawaiensis***		
Cell group	# of cells	Anatomical location		Cell group	# of cells	Anatomical location
Medioposterior	18	rPBp		Medioposterior	20	rPBp
Medial	10	rPBdp		Medial	6	rPBp
Dorsal	8	rHE/MTp		Dorsal	12	rHE/MTd
Medioanterior	2	rMPa		Dorsal-lateral	4	rHE/MTd
Lateroposterior	4	rMTp		Anterior-lateral	2	rHE/MTa
Dorsoanterior	4	rHE/MTa		Anterior-medial a1	2	rMPa
Lateroanterior	2	rLOva		Anterior-medial a2	2	rMPa
Ventroposterior	8-12	rMPp		Anterior-medial b	4	rMPa
				Anterior-medial c	8-10	rMPa

Note: because of its location, the ventroposterior cell group in *E. pulchra* could not be imaged in the time-course studies.

Supplementary Table 2. Statistical tests for all gene-cell group combinations for the HCR-FISH time-course experiment of tidally active, beach-collected *E. pulchra* under LD. Effect size quantified as eta squared. Related to Figure 3 and Supplementary Figure 8. KW: Kruskal-Wallis test. Cell groups with statistically significant periodicities.

Gene	Cell group	Significant variation with time					24-h rhythmicity		12-h rhythmicity	
		Test	df	Test statistic	p-value	Effect size	JTK_cycle	RAIN	JTK_cycle	RAIN
Epper	all clock cells	ANOVA	12	2.590	0.011	0.425	0.003	0.001	1.000	0.852
	medioposterior	ANOVA	12	2.522	0.014	0.431	<0.001	0.001	1.000	0.990
	medial	ANOVA	12	2.617	0.011	0.428	0.022	0.003	1.000	0.711
	large-dorsal	ANOVA	12	2.090	0.041	0.391	0.003	0.192	1.000	1.000
	lateroanterior	KW	12	20.792	0.054	0.187				
	lateroposterior	ANOVA	12	2.200	0.030	0.386	0.459	1.000	1.000	0.999
	dorsoanterior	ANOVA	12	2.346	0.020	0.390	0.602	1.000	0.943	1.000
	dorsal	ANOVA	12	1.718	0.100	0.346				
Epcry2	all clock cells	KW	12	24.662	0.017	0.301	<0.001	<0.001	1.000	0.747
	medioposterior	ANOVA	12	2.563	0.013	0.435	<0.001	<0.001	1.000	0.886
	medial	KW	12	19.532	0.076	0.179				
	large-dorsal	KW	12	26.095	0.010	0.361	<0.001	0.017	1.000	0.996
	lateroanterior	KW	12	18.405	0.104	0.133				
	lateroposterior	KW	12	19.553	0.076	0.176				
	dorsoanterior	KW	12	14.737	0.256	0.061				
	dorsal	KW	12	16.606	0.165	0.118				

Supplementary Table 2. Continued.

Gene	Cell group	Significant variation with time					24-h rhythmicity		12-h rhythmicity	
		Test	df	Test statistic	p-value	Effect size	JTK_cycle	RAIN	JTK_cycle	RAIN
Eptim	all clock cells	KW	12	26.588	0.009	0.347	0.034	0.009	0.034	0.008
	medioposterior	KW	12	20.747	0.054	0.219				
	medial	KW	12	29.999	0.003	0.429	0.170	0.028	0.046	0.005
	large-dorsal	KW	12	17.331	0.138	0.137				
	lateroanterior	KW	12	40.436	<0.001	0.592	0.005	0.001	0.092	0.002
	lateroposterior	KW	12	31.599	0.002	0.456	0.556	1.000	0.009	0.042
	dorsoanterior	KW	12	30.541	0.002	0.412	0.539	0.545	0.169	0.050
	dorsal	KW	12	19.182	0.084	0.184				

Supplementary Table 3. Statistical tests and cosinor analysis (with defined periods of 24-h and/or 12.4-h, whenever appropriate) for all gene-cell group combinations for the HCR-FISH time-course experiment of *P. hawaiensis* entrained to tidal phase θ. Related to Figure 4 and Supplementary Table 7. Effect size quantified as eta squared. Phase derived from cosinor fit is corrected to Circadian Time (CT) =0 or Circatidal Time (CTT) =0, as appropriate. KW: Kruskal-Wallis test; RAE: relative amplitude error. Cell groups with statistically significant periodicities.

Gene	Cell group	Significant variation with time					24-h rhythmicity		12-h rhythmicity		Cosinor fit	
		Test	df	Test statistic	p-value	Effect size	JTK_cycle	RAIN	JTK_cycle	RAIN	phase	RAE
Phper	all clock cells	ANOVA	8	11.99	<0.001	0.813	<0.001	<0.001	0.299	0.083	22.33	0.16
	medioposterior	ANOVA	8	62.35	<0.001	0.954	<0.001	<0.001	0.381	0.262	22.32	0.07
	anterior-medial a1	ANOVA	8	43.95	<0.001	0.934	<0.001	<0.001	0.388	0.793	22.31	0.06
	anterior-medial b	ANOVA	8	2.253	0.059	0.429						
	anterior-medial c	ANOVA	8	1.856	0.125	0.426						
	dorsal	ANOVA	8	1.962	0.099	0.406						
	anterior-lateral	ANOVA	8	1.090	0.403	0.267						
	anterior-medial a2	ANOVA	8	2.157	0.068	0.408						
	medial-1	ANOVA	8	1.031	0.441	0.256						
	medial-2	ANOVA	8	1.180	0.353	0.291						
	dorsal-lateral	ANOVA	8	6.584	<0.001	0.678	1	0.034	0.006	<0.001	4.20	0.18
Phcry2	all clock cells	ANOVA	8	3.942	0.005	0.589	0.441	0.023	0.087	0.004		
	medioposterior	ANOVA	8	15.13	<0.001	0.835	<0.001	<0.001	0.059	0.002	9.35	0.14
	anterior-medial a1	ANOVA	8	9.814	<0.001	0.758	<0.001	<0.001	0.930	0.567	8.86	0.14
	anterior-medial b	ANOVA	8	1.501	0.209	0.333						
	anterior-medial c	KW	8	7.572	0.476	−0.021						
	dorsal	ANOVA	8	1.391	0.252	0.326						
	anterior-lateral	ANOVA	8	0.7758	0.628	0.205						
	anterior-medial a2	ANOVA	8	0.4122	0.903	0.117						
	medial-1	ANOVA	8	1.387	0.252	0.316						
	medial-2	KW	8	8.827	0.357	0.036						
	dorsal-lateral	ANOVA	8	6.866	<0.001	0.687	1	0.086	0.002	<0.001	5.26	0.18

Supplementary Table 4. Statistical tests and cosinor analysis (with defined periods of 24-h and/ or 12.4-h, whenever appropriate) for all gene-cell group combinations for the HCR-FISH time-course experiment of *Parhyale hawaiensis* entrained to tidal phase θ +1.2 h. Related to Figure 5, Supplementary Figure 10 and Supplementary Table 7. Effect size quantified as eta squared. Phase derived from cosinor fit is corrected to Circadian Time (CT) =0 or Circatidal Time (CTT) =0, as appropriate. KW: Kruskal-Wallis test; RAE: relative amplitude error. Cell groups with statistically significant periodicities.

Gene	Cell group	Significant variation with time					24-h rhythmicity		12-h rhythmicity		Cosinor fit	
		Test	df	Test statistic	p-value	Effect size	JTK_cycle	RAIN	JTK_cycle	RAIN	phase	RAE
Phper	all clock cells	ANOVA	8	4.899	0.003	0.697	<0.001	<0.001	1	<0.001	23.03	0.17
	medioposterior	ANOVA	8	12.96	<0.001	0.845	<0.001	<0.001	0.772	0.462	22.90	0.11
	anterior-medial a1	ANOVA	8	49.29	<0.001	0.952	<0.001	<0.001	1	0.753	22.17	0.06
	anterior-medial b	KW	8	16.20	0.040	0.304	0.232	0.003	0.772	0.106		
	anterior-medial c	ANOVA	8	1.101	0.414	0.370						
	dorsal	ANOVA	8	0.7518	0.648	0.273						
	anterior-lateral	ANOVA	8	1.982	0.109	0.468						
	anterior-medial a2	ANOVA	8	1.732	0.152	0.410						
	medial-1	ANOVA	8	0.5012	0.84	0.182						
	medial-2	ANOVA	8	0.4058	0.902	0.160						
	dorsal-lateral	ANOVA	8	7.212	<0.001	0.743	0.232	0.003	0.016	<0.001	4.53	0.21
Phcry2	all clock cells	ANOVA	8	1.266	0.323	0.373						
	medioposterior	ANOVA	8	7.967	<0.001	0.770	0.005	<0.001	0.023	0.001	7.01	0.24
	anterior-medial a1	ANOVA	8	6.807	<0.001	0.731	<0.001	<0.001	1	0.773	7.88	0.13
	anterior-medial b	ANOVA	8	2.880	0.026	0.535	0.222	0.014	1	0.460		
	anterior-medial c	ANOVA	8	0.4578	0.867	0.196						
	dorsal	ANOVA	8	0.9256	0.522	0.316						
	anterior-lateral	ANOVA	8	0.5485	0.805	0.196						
	anterior-medial a2	ANOVA	8	1.667	0.168	0.400						
	medial-1	ANOVA	8	0.6999	0.688	0.237						
	medial-2	ANOVA	8	1.522	0.222	0.417						
	dorsal-lateral	ANOVA	8	4.908	0.002	0.663	1	0.215	0.016	<0.001	6.58	0.18

Supplementary Table 5. Statistical tests and cosinor analysis (with defined periods of 24-h and/ or 12.4-h, whenever appropriate) for all gene-cell group combinations for the HCR-FISH time-course experiment of *P. hawaiensis* entrained to tidal phase θ – 5.4 h. Related to Figure 5, Supplementary Figure 11 and Supplementary Table 7. Effect size quantified as eta squared. Phase derived from cosinor fit is corrected to Circadian Time (CT) =0 or Circatidal Time (CTT) =0, as appropriate. KW: Kruskal-Wallis test; RAE: relative amplitude error. Cell groups with statistically significant periodicities.

Ge	Cell group	Significant variation with time					24-h rhythmicity		12-h rhythmicity		Cosinor fit	
		Test	df	Test statistic	p-value	Effect size	JTK_cycle	RAIN	JTK_cycle	RAIN	phase	RAE
Phper	all clock cells	KW	8	19.98	0.010	0.705	0.002	<0.001	0.627	0.25	22.32	0.16
	medioposterior	KW	8	20.39	0.009	0.689	0.002	<0.001	1	0.879	22.57	0.11
	anterior-medial a1	ANOVA	8	23.67	<0.001	0.913	0.005	<0.001	0.829	0.654	22.73	0.12
	anterior-medial b	ANOVA	8	1.912	0.121	0.096						
	anterior-medial c	KW	8	9.893	0.273	0.111						
	dorsal	ANOVA	8	1.808	0.145	0.460						
	anterior-lateral	KW	8	11.99	0.152	0.234						
	anterior-medial a2	KW	8	6.759	0.563	−0.073						
	medial-1	KW	8	11.56	0.172	0.223						
	medial-2	KW	8	7.392	0.495	-0.036						
	dorsal-lateral	ANOVA	8	7.469	<0.001	0.768	1	0.277	<0.001	<0.001	4.40	0.15
Phcry2	all clock cells	ANOVA	8	1.544	0.215	0.421						
	medioposterior	ANOVA	8	2.537	0.048	0.530	0.016	0.001	1	0.84	9.06	0.23
	anterior-medial a1	KW	8	10.06	0.261	0.114						
	anterior-medial b	ANOVA	8	1.129	0.391	0.334						
	anterior-medial c	ANOVA	8	2.131	0.090	0.501						
	medial-1	ANOVA	8	1.497	0.234	0.428						
	medial-2	ANOVA	8	0.8941	0.542	0.296						
	dorsal	KW	8	13.51	0.096	0.324						
	anterior-lateral	ANOVA	8	4.823	0.003	0.694	1	0.203	<0.001	<0.001	3.93	0.17
	anterior-medial a2	KW	8	12.26	0.14	0.251						
	dorsal-lateral	ANOVA	8	8.943	<0.001	0.799	0.758	0.085	<0.001	<0.001	5.59	0.18

Supplementary Table 6. Statistical tests and cosinor analysis (with defined periods of 24-h whenever appropriate) for all gene-cell group combinations for the HCR-FISH time-course experiment of *P. hawaiensis* synchronised to and sampled under LD. Related to Figure 6 and Supplementary Figure 14. Effect size quantified as eta squared. Phase derived from cosinor fit is corrected to Circadian Time (CT) =0. KW: Kruskal-Wallis test; RAE: relative amplitude error. Cell groups with statistically significant periodicities.

G	Cell group	Significant variation with time					24-h rhythmicity		12-h rhythmicity		Cosinor fit	
		Test	df	Test statistic	p-value	Effect size	JTK_cycle	RAIN	JTK_cycle	RAIN	phase	RAE
Phper	all clock cells	ANOVA	12	14.28	<0.001	0.764	<0.001	<0.001	1	0.250	21.14	0.11
	medioposterior	KW	12	54.45	<0.001	0.801	<0.001	<0.001	1	0.515	21.62	0.07
	anterior-medial a1	KW	12	57.04	<0.001	0.850	<0.001	<0.001	1	0.717	21.05	0.09
	anterior-medial b	ANOVA	12	9.073	<0.001	0.673	<0.001	<0.001	1	0.791	21.55	0.11
	anterior-medial c	ANOVA	12	1.697	0.095	0.285						
	dorsal	ANOVA	12	6.225	<0.001	0.585	<0.001	<0.001	1	0.193	19.11	0.18
	anterior-lateral	KW	12	13.09	0.363	0.021						
	anterior-medial a2	KW	12	20.94	0.051	0.172						
	medial-1	KW	12	24.66	0.017	0.239	1	0.868	1	0.014		
	medial-2	KW	12	20.18	0.064	0.157						
	dorsal-lateral	ANOVA	12	3.973	<0.001	0.474	0.103	0.003	1	0.051		
Phcry2	all clock cells	KW	12	26.16	0.010	0.267	0.05	0.001	1	0.019	11.70	0.36
	medioposterior	ANOVA	12	12.40	<0.001	0.737	<0.001	<0.001	0.014	<0.001	9.03	0.16
	anterior-medial a1	KW	12	41.79	<0.001	0.562	<0.001	<0.001	1	0.219	8.28	0.12
	anterior-medial b	ANOVA	12	6.574	<0.001	0.598	<0.001	<0.001	1	0.580	16.39	0.14
	anterior-medial c	ANOVA	12	2.203	0.026	0.341	0.049	0.009	1	0.034	15.78	0.34
	dorsal	ANOVA	12	1.792	0.074	0.289						
	anterior-lateral	ANOVA	12	0.9371	0.518	0.178						
	anterior-medial a2	KW	12	15.15	0.233	0.061						
	medial-1	ANOVA	12	1.233	0.286	0.218						
	medial-2	ANOVA	12	2.057	0.037	0.322	1	0.951	1	0.989		
	dorsal-lateral	ANOVA	12	1.501	0.153	0.254						

Supplementary Table 7. Circular statistics of gene-cell group combinations that show statistically significant rhythmicity (at 24-h or 12-h) across 3 HCR-FISH time-course experiments of tidally entrained *P. hawaiensis*. Related to Figure 7, Supplementary Figures 10, 11, Supplementary Tables 4-6.

Gene	Cell group	Mean phase	Mean vector length	Number of experiments
Circadian oscillations				
Phper	All clock cells	22.56	1.00	3
	Medioposterior	22.60	1.00	3
	Anterior-medial a1	22.40	1.00	3
Phcry2	Medioposterior	8.48	0.96	3
	Anterior-medial a1	8.37	0.99	2
Circatidal oscillations				
Phper	Dorsal-lateral	4.38	1.00	3
Phcry2		5.81	0.96	3

Supplementary Table 8. The targets, hairpin identities and lot numbers of the HCR-FISH primary probes used to generate the data described in this study.

Probe/target genes	NCBI accession #	Probe hairpin	Number of probe pairs	Lot number	Relevant figure(s)
EpBmal1	KC885968.1	B3	20	PRP939	Fig. 1, Supp. Fig. 3-4
EpBmal1 additional	KC885968.1	B3	40	RTA402	Fig. 1, Supp. Fig. 3-4
EpClk 1-9	KC885973.1	B1	40	RTA400	Fig. 1, Supp. Fig. 3
EpClk 1-9 additional	KC885973.1	B1	29	RTE285	Fig. 1, Supp. Fig. 3
Epcry2	KC885970.1	B1	20	RTA399	Fig. 1, Supp. Fig. 3, 6
Epcry2	KC885970.1	B3	20	RTO453	Fig. 1, Supp. Fig. 8
Epper	KC885967.1	B2	20	RTO454	Fig. 1, 3, Supp. Fig. 3, 8
Eptim	KC885969.1	B1	20	PRP937	Fig. 1, 3, Supp. Fig. 3, 8
PhBmal1	Not applicable. Sequences from Hunt, Mallon & Rosato (2019)	B1	38	RTC080	Fig. 1, Supp. Fig. 3-4
Phpdh		B1	12	RTF908	Fig. 1, Supp. Fig. 3
Phper		B1/B2	30	RTK407/RTC082	Fig. 1, 4-6, Supp. Fig. 3, 10-11, 13
PhClk-fragment 1		B2	40	RTG497	Fig. 1, 4-6, Supp. Fig. 3, 6, 10-11, 13
PhClk-fragment 2		B2	28	RTG498	Fig. 1, 4-6, Supp. Fig. 3, 10-11, 13
Phcry2		B3	30	RTC083	Fig. 1, 4-6, Supp. Fig. 3, 6, 10-11, 13
deGFP	Not applicable. Sequence provided by Molecular Instruments Inc.	B1	12	RTA210	Supp. Fig. 3
deGFP		B2	12	PRQ740	Supp. Fig. 3

Supplementary Table 9. The names, hairpin identities and lot numbers of the RNAScope technology FISH probes

Probe/target gene	**NCBI accession #**	**Amplifier**	**ACD cat number**
Epper-C4	KC885967.1	C4	578211-C4
EpClk5-C1	KC885973.1	C1	578151-C1
Epcry2-C1	KC885970.1	C1	1039411-C1
Eptim-C3	KC885969.1	C3	1099401-C3
EpBmal1-C2	KC885968.1	C2	578191-C2
-ve control			

* Negative control probe is designed against the DapB gene of *Bacillus subtilis* strain

Supplementary Table 10. FISH time-course designs for investigating clock gene expression rhythms. Related to Supplementary Figure 15.

Experiment	Sampling condition	First sampling time-point	*N* total animals sampled	Sampling interval	1st subjective high tide onset during sampling	HCR-FISH primary probes	HCR-FISH hairpins (AF: AlexaFluor)	Relevant figures/tables
14h:10h LD-maintained *E. pulchra* (Supp. Fig. 15A)								
LD (*E. pulchra*)	LD	ZT7	65	2	ZT18.4	*Eptim*-B1, *Epper*-B2, *Epcry2*-B3	B1-AF647, B2-AF546, B3-AF488	Fig. 3, Supp. Fig. 8, Supp. Table 2
Tidally entrained *P. hawaiensis* (Supp. Fig. 15B)								
Tidal θ *P. hawaiensis*	DD	CT0	37	3	CT9.2	*Phper*-B2, *Phcry2*-B3	B2-AF546, B3-AF488,	Fig. 4, Supp. Table 3
Tidal θ + 1.2h *P. hawaiensis*	DD	CT0	35	3	CT10.4	*Phper*-B2, *Phcry2*-B3	B2-AF647, B3-AF488,	Fig. 5, Supp. Fig. 10, Supp. Table 4
Tidal θ – 5.4h *P. hawaiensis*	DD	CT0	35	3	CT3.8	*Phper*-B2, *Phcry2*-B3	B2-AF647, B3-AF488,	Fig. 5, Supp. Fig. 11, Supp. Table 5
12h:12h LD-synchronised *P. hawaiensis* (Supp. Fig. 15C)								
LD (*P. hawaiensis*)	LD	ZT1	79	2	N.A.	*Phper*-B1, *PhClk*-fragment1-B2, *PhClk*-fragment2-B2, *Phcry2*-B3	B1-AF647, B2-AF546, B4-AF647	Fig. 6, Supp. Figs. 13, Supp. Table 6

Supplementary Results

Neuropils of *E. pulchra*.

In *E. pulchra*, the optic neuropils comprise lamina (LA), medulla (ME), and lobula (LO). The ME is proximal to the LA and distal to the LO. Ventral to the LO is a small unidentified neuropil. The optic neuropils are distal to the lateral protocerebrum (LP), which comprises the medulla terminalis (MT) and hemi-ellipsoid body (HE). These neuropils are poorly demarcated, and we did not attempt to determine the borders of each, segmenting them as a contiguous complex (HE/MT). The median protocerebrum (MP) comprises a large central body (CB) and protocerebral bridge (PB). The CB extends across the width of the brain and appears to be layered. Ventral to the protocerebrum is the deutocerebrum comprising the deutocerebral chemosensory lobes (DCL) and lateral antenna 1 neuropil (LAN). The DCL are lateral to the brain and comprise numerous olfactory glomeruli. Medial of the DCL is the LAN and ventral of this is antenna 2 neuropil (ANN) within the tritocerebrum. We also identified lateral accessory lobes (LAL) and nodules (NOD), and the medial antenna 1 neuropil (MAN). For *P. hawaiensis* we confirmed the anatomy of Whittforth et al. [1] and identified all major neuropils in our refence brain, which correspond closely with those we describe in *E. pulchra*. See also Supplementary Figures 4-5 and Supplementary Videos 1-2.

Cell groups of *E. pulchra* and *P. hawaiensis*

In *E. pulchra, per-* and *cry2*-expressing cells were primarily found in the posterior cell body rind overlying the medial protocerebrum (MP), hemi-ellipsoid body and medulla terminalis (HE/MT, Figure 4a, b). There were nine somata in the rind posterior to the protocerebral bridge (rPBp) [2], which we termed the “medioposterior” cells. Dorsal and anterior to these cells was a cluster of 5 somata in the cell body rind dorsal to the PB (rPBd) that we assigned as “medial” cells. Lateral to these medial and medioposterior cells was a cell pair in the rind posterior of the medulla terminalis (rMTp) which we named “lateroposterior” cells. In the cell body rind posterior to the hemi-ellipsoid body/ medulla terminalis (rHEp/MTp) were 4 “dorsal” cells, one of which was larger than the others and we refer to as “large dorsal” cell. In the dorsal region of the cell body rind posterior of the MP (rMPp) ~4-6 “ventroposterior” cells. In the anterior aspect of the brain, we found fewer cells; in the cell body rind lateroanterior of the hemi-ellipsoid body/medulla terminalis (rHE/MTla) was a single pair of cells, the “dorsoanterior” cells. A single “lateroanterior” cell was in the rind ventral and anterior of the lobula (rLOva). Finally, a pair of cells on the midline (one per hemisphere), anterior of the medial protocerebrum were named “medioanterior” cells (rMPa). Cell groups and their given nomenclature are summarised in Supplementary Table 1.

In *P. hawaiensis*, *per*- and *cry2*-enriched cells were found throughout the anterior and posterior aspects of cell body rind overlying MP and HE/MT. In the cell body rind posterior and lateral to the PB (rPBp) were ten *per*- and *cry2*-enriched somata that we assigned as “medioposterior” cells (Figure 4c, d). Dorsoanterior to these cells were three cells, two of which were closer to each other than the last one; these we termed “medial-2” and “medial-1”, respectively, and collectively, the medial cells. In the cell body rind dorsal of the HE/MT (rHE/MTd), we identified two somata as the “dorsal-lateral” cells, and antero-medial to these cells were six cells that we called the “dorsal” cells. On the anterior aspect of the brain, we identified one cell in the cell body rind anterior of the HE/MT (rHE/MTa) as “anterior-lateral” cells. Lastly, we found 8 – 9 cells on the anterior aspect of the medial protocerebrum (rPMa). We refer to these cells collectively as the “anterior-medial” cells and they can be divided into 4 groups. “Anterior-medial b” cells described two cells with distinctive location lateral to the myoarterial formation. Dorsal to the anterior-medial b cells were two cells, in which one was positioned medially to the other. These, we termed “anterior-medial a1” and “anterior-medial a2” cells, respectively. The “anterior-medial c” cells were a group of 4 – 5 cells located dorsal to the anterior-medial a1-2 cells.

Supplementary Video 1

Reference brain of *E. pulchra* revealed by anti-SYNORF1 immunostaining and neuroanatomy of putative clock cell groups revealed by co-immuno-HCR-FISH staining.

Related to Figure 4a and Supplementary Figure 5a.

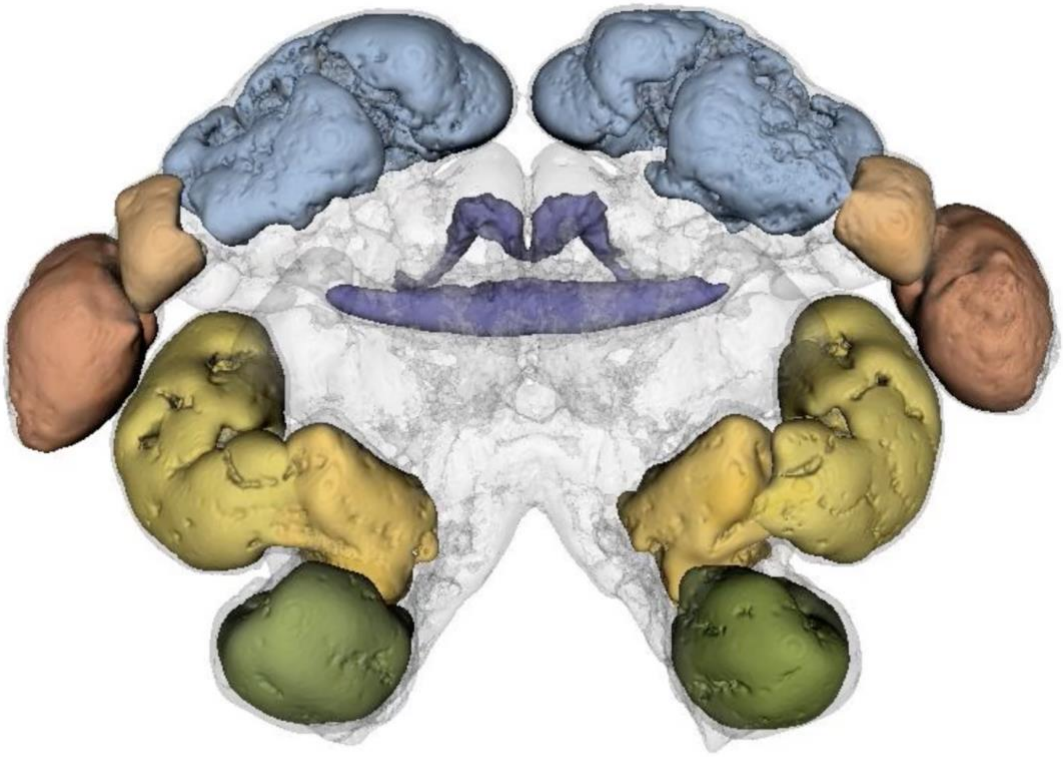

Supplementary Video 2

Reference brain of *P. hawaiensis* revealed by anti-SYNORF1 immunostaining and neuroanatomy of putative clock cell groups revealed by co-immuno-HCR-FISH staining.

Related to Figure 4c and Supplementary Figure 5 c.

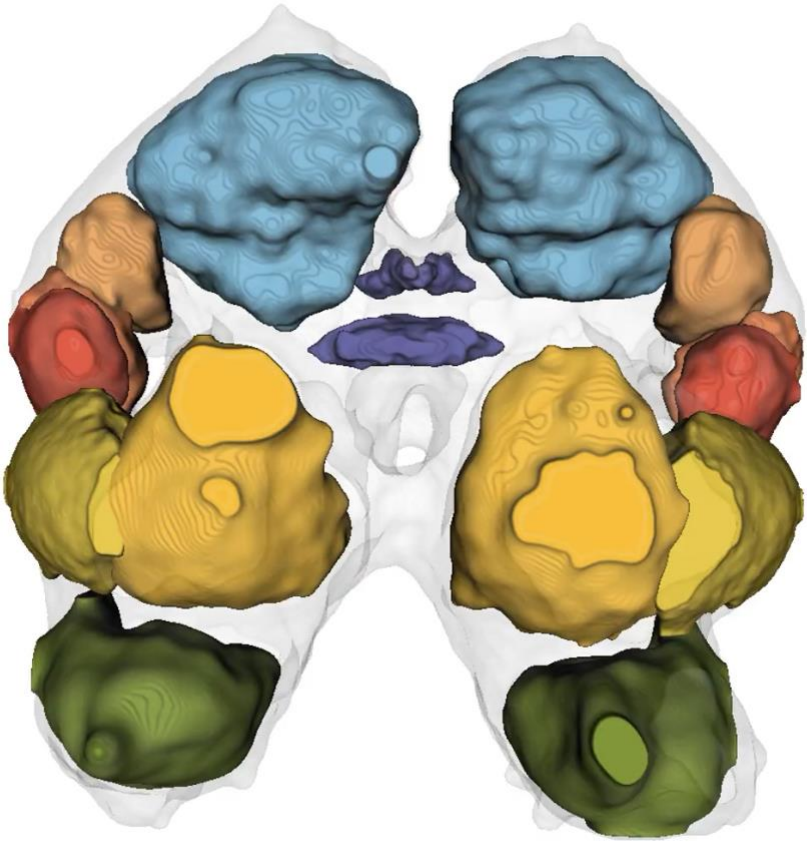

97 **Supplementary methods**

98

99 ***Immunostaining***

100 For immunolabelling of *E. pulchra* brains with anti-SYNORF1, after rehydration to PBST,
101 brains were washed in PTx (PBS supplemented with 0.1% Triton X-100), permeabilised in
102 detergent solution (50 mM Tris-HCl pH 7.5, 150 mM NaCl, 1 mM EDTA pH 8, 1% SDS, 0.5%
103 Tween-20) for 30 min at room temperature (Bruce et al. 2021) and then incubated with 1:50
104 anti-SYNORF1 in PTx containing 5% normal goat serum (NGS) overnight at room
105 temperature, followed by 5 days at 4°C, with rotation. After extensive washing in PTx, brains
106 were incubated with anti-mouse Alexa 488 (ThermoFisher #A-21141) at 1:1000 in PTx
107 containing 5% NGS for 3 days at 4°C, with rotation. After extensive washing with PTx, nuclei
108 were stained with 0.1 µg/mL DAPI int PTx for 1h. Brains were then bridge-mounted in
109 RapiClear 1.49 (SunJin Lab Optical Clearing Innovation, #RC149001) using No. 2 thickness
110 coverslips to maintain 3D morphology. For *P. hawaiensis*, brains were incubated in blocking
111 buffer (1x PBS, 0.5% Tween-20, 5% NGS, 1% bovine serum albumin) containing 1:50 anti-
112 SYNORF1 for 3 days at 4°C with gentle shaking, followed by extensive washing in PTw (PBS
113 supplemented with 0.5% Tween-20) and incubation in secondary antiserum F(ab')2-goat anti-
114 mouse IgG-Alexa Fluor 488 (ThermoFisher #A-11017) or Alexa Fluor Plus 555 (ThermoFisher
115 #A48287) at 1:250 made in blocking buffer for 2 days at 4°C with gentle agitation. Nuclei were
116 stained with 0.1 µg/mL DAPI for 30 min prior to final washing in PTw and preparations
117 mounted in DPX (Sigma Aldrich #06522) according to [3].

118

119 ***Reference brains***

120 Whole-mount brain samples used for generating reference brains and describing the
121 neuroanatomy of putative clock cells were imaged on a Nikon CSU-W1 spinning disk confocal
122 microscope equipped with a 25x/1.05NA silicone oil CFI Plan Apochromat Lambda S objective
123 and a Prime 95B 22mm sCMOS camera. To make an *E. pulchra* reference brain, two sex-
124 specific references were made by registering and then averaging 7 male brains to one male
125 "seed" brain and 6 female brains to a female "seed" brain. These sex-specific references were
126 then averaged to generate a final intersex reference brain (an average of 15 brains) used for
127 all subsequent analyses. For *P. hawaiensis*, 10 male brains were registered and then
128 averaged to a seed brain to generate a reference brain. Registration and averaging were
129 done using: https://github.com/jefferislab/MakeAverageBrain [4] [5]. Briefly, Computational
130 Morphometry Toolkit (CMTK) was used to register image stacks against a seed image stack;
131 first with a rigid and then a non-rigid registration [6,7]. Image stacks of brains with co-immuno-
132 RNA-FISH labelling of neuropils and circadian clock genes (*per*/ *cry2*/ *tim*) were registered to

133 reference brains based on the anti-SYNORF1 signal. Three-dimensional surface models of
134 neuropils were based on reference brains and generated using the Segmentation Editor in
135 3DSlicer software (www.slicer.org). 3D surface models of putative clock cells were based on
136 circadian clock gene HCR-FISH labelling (*Epcry2* or *Phcry2*) in an image stack registered to
137 the reference brain and using the Segmentation Editor in 3DSlicer.
138
139 ***HCR-FISH***
140 For HCR-FISH, rehydrated brains were permeabilised in detergent solution for 30 min at room
141 temperature, and equilibrated in pre-warmed probe hybridisation buffer for 30 min at 37°C.
142 Brains were then incubated in probe hybridisation solution containing 10 nM of each primary
143 probe set for 2 days (*E. pulchra*) or 3 days (*P. hawaiensis*) at 37°C. For *P. hawaiensis*, 1:1000
144 murine RNase inhibitor (NEB #M0314L) was added to the probe hybridisation buffer. Signal
145 amplification with 60 nM fluorescently tagged hairpins was allowed to proceed for 2 days,
146 followed by staining with 0.1 µg/mL DAPI in 5x SSC supplemented with 0.5% Tween-20 (30
147 min) during one of the final washing steps. *E. pulchra* brains were bridge-mounted using No.
148 1.5 thickness coverslips in RapiClear 1.49 whilst *P. hawaiensis* brains were dehydrated and
149 mounted in DPX according to [3]. The target genes used for probe design, their accession
150 numbers, and the Molecular Instruments probe lot numbers and concentrations used are listed
151 in Supplementary Tables 8. For experiments investigating co-expression of clock genes, a
152 40x/1.3NA Plan Fluorite oil immersion objective was used to image with an optical section
153 interval of 1 µm.
154
155 For co-immuno-RNA-FISH staining, following rehydration and permeabilization in detergent
156 solution, *E. pulchra*, brains were incubated with 1:50 anti-SYNORF1 in PTx containing 1.6
157 U/µL RNaseOUT™ ribonuclease inhibitor (Invitrogen #10777019) overnight at room
158 temperature, followed by 3 days at 4°C, with rotation. After extensive washing in PTx, brains
159 were incubated with anti-mouse Alexa 488 (ThermoFisher #A-21141) at 1:1000 in PTx
160 containing RNase inhibitor for 2 days at 4°C, with rotation. After washing in PTx/w, brains
161 were fixed in 4% PFA (in PBS) for 1 hour at room temperature. After washing in PTx/w, the
162 neuropil-stained brains were processed for HCR-FISH as above and mounted as described
163 above. *P. hawaiensis* brains were washed in PTw and subjected to one-step immunostaining
164 [8] by incubating in PTw containing pre-mixed 1:250 murine RNase inhibitor, 1:50 anti-
165 SYNORF1, 3.33 ng/µL Fab goat anti-mouse IgG-Alexa Fluor 488 (Jackson ImmunoResearch
166 #115-547-003) for 2 days at room temperature.
167
168 **RNAscope methods for formalin-fixed, paraffin-wax embedded *E.pulchra* brains**

169

170 *E. pulchra* brains were dissected in ice-chilled crustacean saline [9] and fixed immediately in
171 10% normal buffered formalin (10%) overnight (16h) at RT. After fixing, brains were washed
172 extensively in PBS, dehydrated through an ethanol series (50%, 70%, 80%, 90%, 95%,
173 100%), cleared in xylene (1h at RT) and infiltrated in molten wax (Leica Paraplast Plus®, Leica
174 Biosystems, Sheffield UK) 3x, each for 1h, before embedding in wax such that the brains could
175 be mounted for frontal sections to be cut. Serial sections (6µm) were cut on a standard wax
176 microtome and mounted on Superfrost™ Plus (Thermo Fisher, UK). After drying, sections
177 were baked at 60°C for 2h to adhere fully to the slides. Slides were de-waxed in clean xylene
178 and taken to water through an ethanol series before drying at 60C for 1h. Following
179 preparation, manufacturer's instructions were followed exactly, except that target retrieval was
180 done in 700 mL Target Retrieval buffer in a 1L beaker, for 15 minutes at 98-104°C, over a hot-
181 plate. Protease Plus was applied for 30 minutes at 40°C. Signal amplification was done using
182 Opal™ fluors (Opal 520 and Opal 570). All reagents and kit components were as
183 recommended by ACD Biotechne (Abingdon, Oxford, UK. RNAscope® Multiplex Fluorescent
184 Reagent Kit v2 Assay). Target probes were designed by ACD Biotechne and probe details
185 provided in Supplementary Tables 9. Negative control probes were supplied by ACD
186 Biotechne and are designed against the *DapB2* gene of *Bacillus subtilis.* Following
187 hybridisation and amplification, sections were counterstained with DAPI provided with the kit
188 and mounted under Vectashield® Antifade mounting fluid (Vector Laboratories, supplied by
189 2B Scientific, Oxford, UK). Images were captured on a Leica SP8 confocal microscope at
190 1µm z-stack intervals and using Leica LAX proprietary software. Images were re-sized,
191 cropped and adjusted for brightness and contrast using ImageJ software.

192

193

Supplementary References

1. Wittfoth, C., Harzsch, S., Wolff, C., and Sombke, A. (2019). The "amphi"-brains of amphipods: new insights from the neuroanatomy of *Parhyale hawaiensis* (Dana, 1853). Front Zool *16*, 30. 10.1186/s12983-019-0330-0.
2. Ito, K., Shinomiya, K., Ito, M., Armstrong, J.D., Boyan, G., Hartenstein, V., Harzsch, S., Heisenberg, M., Homberg, U., Jenett, A., et al. (2014). A systematic nomenclature for the insect brain. Neuron *81*, 755-765. 10.1016/j.neuron.2013.12.017.
3. Meissner, G.W., Grimm, J.B., Johnston, R.M., Sutcliffe, B., Ng, J., Jefferis, G.S.X.E., Cachero, S., Lavis, L.D., and Malkesman, O. (2018). DPX Mounting of Drosophila CNS. protocols.io. dx.doi.org/10.17504/protocols.io.qj2duqe.
4. Costa, M., Manton, J.D., Ostrovsky, A.D., Prohaska, S., and Jefferis, G.S. (2016). NBLAST: Rapid, Sensitive Comparison of Neuronal Structure and Construction of Neuron Family Databases. Neuron *91*, 293-311. 10.1016/j.neuron.2016.06.012.
5. Bates, A.S., Manton, J.D., Jagannathan, S.R., Costa, M., Schlegel, P., Rohlfing, T., and Jefferis, G.S. (2020). The natverse, a versatile toolbox for combining and analysing neuroanatomical data. Elife *9*. 10.7554/eLife.53350.
6. Jefferis, G.S.X.E., Potter, C.J., Chan, A.M., Marin, E.C., Rohlfing, T., Maurer, C.R., Jr., and Luo, L. (2007). Comprehensive Maps of Drosophila Higher Olfactory Centers: Spatially Segregated Fruit and Pheromone Representation. Cell *128*, 1187-1203. 10.1016/j.cell.2007.01.040.
7. Rohlfing, T., and Maurer, C.R., Jr. (2003). Nonrigid image registration in shared-memory multiprocessor environments with application to brains, breasts, and bees. IEEE Trans Inf Technol Biomed *7*, 16-25. 10.1109/titb.2003.808506.
8. Wang, S. (2019). Single Molecule RNA FISH (smFISH) in Whole-Mount Mouse Embryonic Organs. Current Protocols in Cell Biology *83*. 10.1002/cpcb.79.
9. Saver, M.A., Wilkens, J.L., and Syed, N.I. (1999). In Situ and In Vitro Identification and Characterization of Cardiac Ganglion Neurons in the Crab, *Carcinus maenas*. Journal of Neurophysiology *81*, 2964-2976. 10.1152/jn.1999.81.6.2964.